Dynamic tradable credit scheme for multimodal urban networks

Louis Balzer, Mostafa Ameli, Ludovic Leclercq, Jean-Patrick Lebacque

Transportation Research Part C 149 (2023) 104061

Contents lists available at ScienceDirect

Transportation Research Part C

journal homepage: www.elsevier.com/locate/trc

Dynamic tradable credit scheme for multimodal urban networks

Louis Balzer [a], Mostafa Ameli [b], Ludovic Leclercq [a,*], Jean-Patrick Lebacque [b]

[a] Univ Gustave Eiffel, Univ Lyon, ENTPE, LICIT-ECO7, F-69675 Lyon, France
[b] Univ Gustave Eiffel, GRETTIA, F-77454 Paris, France

ARTICLE INFO

Keywords:
Generalized bathtub
Tradable credit scheme
Mode choice
Departure time

ABSTRACT

A Tradable Credit Scheme (TCS) is a demand management policy aiming for more sustainable travel behavior. The regulator defines the total credit cap and the credit distribution; it also determines the credit charges for each travel alternative at different times of the day, which modifies the perceived users' costs. The credit price is determined by trading of credits between travelers. Defining the credit scheme at the urban level and estimating its impacts on user travel decisions and the network congestion dynamics is challenging. We propose a framework wherein travelers change their departure times and choose between solo car driving, Public Transportation (PT), and carpooling to complete their trips under a dynamic TCS, meaning the credit charge is time-dependent. A multimodal macroscopic traffic simulator based on a generalized bathtub model captures the congestion dynamics for the different transport modes. Additionally, we consider different values of time, trip lengths, and desired arrival times for the demand profile.

The proposed TCS minimizes the total travel cost, (the sum of all travelers' travel costs) and the carbon emissions by solving an optimization problem through an iterative method, including an inner loop that updates the users' choices and credit price under the stochastic user equilibrium principle; and an outer loop that updates the credit charge profile. The methodology is implemented and applied to a realistic test case in Lyon (France). The dynamic TCS profiles result in 36% fewer carbon emissions than static TCS for a total travel cost reduction of 19%. Besides, 94% of the travelers benefit from the TCS as their user costs decrease in the case study. The final results are compared with a more advanced simulation framework, which is too computationally expensive to find the optimal TCS. The proposed TCS is effective with refined traffic dynamics representation.

1. Introduction

Automotive congestion has been an issue for many cities worldwide for decades. The traffic engineering and transportation economics communities have proposed different demand management approaches to foster shifting demand to off-peak periods and sustainable transportation modes. A Tradable Credit Scheme (TCS) is a quantity-based framework that introduces a commodity for traveling: credits. The regulator issues and distributes credits to travelers. Depending on the departure time and transportation mode, a traveler must spend credits to access the transportation network. The credits can be traded between travelers through a dedicated marketplace. The supply and demand for credits are linked to the travel times of the different travel alternatives. Thus, estimating congestion over the scale of a city is essential. Also, the design of the TCS, especially the number of credits needed for the different travel options, is linked to the goals the regulator wants to achieve. The objective function used most is related to the economic

* Corresponding author.
E-mail address: ludovic.leclercq@univ-eiffel.fr (L. Leclercq).

https://doi.org/10.1016/j.trc.2023.104061
Received 16 September 2022; Received in revised form 15 February 2023; Accepted 15 February 2023
Available online 1 March 2023

aspect of congestion: the total travel time or cost. It represents the time and money lost due to congestion. Other objectives linked to the environmental footprint of the transportation network, like the emissions of pollutants, can also be considered. However, reducing congestion or pollution might lead to different TCS, and trade-offs must be found. In this context, our contribution is to address this trade-off by setting up an advanced multimodal congestion model and an optimization framework. We proceed with a literature review on traffic congestion models and multimodality in TCS frameworks.

1.1. Congestion models

The problem of peak-hour congestion, i.e., when the travel demand exceeds the capacity for specific time periods, has been investigated for more than half a century (Li et al., 2020). Different congestion models have been proposed and consequently improved. The most common model in the literature of macroscopic traffic models is *Vickrey's bottleneck*. Vickrey (1969) represented the congestion as a point queue with a fixed capacity. The queue disappears by implementing marginal cost pricing, and the total travel cost is reduced by a factor of two. In 1991, Vickrey relaxed the fixed capacity assumption (Vickrey, 2020) (work published posthumously) with a new model, named the *classical bathtub model*. The main idea is to define the network as an undifferentiated movement area with a mean speed function. The mean speed is defined as a function of network density and network characteristics (Fosgerau and Small, 2013; Arnott, 2013). Therefore, the network speed decreases as demand increases. Fosgerau (2015) extended the framework to account for different desired arrival times. Arnott and Buli (2018) proposed a numerical framework for determining the departure times distribution. Mariotte et al. (2017) and Leclercq et al. (2017) introduced the trip-based Macroscopic Fundamental Diagram (MFD) to consider any trip length distribution. The mean speed is a function of vehicle accumulation, which is the key state variable of the classical bathtub and MFD models. Lamotte and Geroliminis (2018) described a numerical resolution method to compute the departure times distribution at equilibrium. Jin (2020) introduced an extension for the classical bathtub model, named *generalized bathtub*. The author presented a numerical framework for computing travel times. The key state variable is the distribution of the remaining trip lengths of the travelers, which was also introduced in Lamotte and Geroliminis (2018). However, departure time optimization was not addressed. Recently, Ameli et al. (2022) applied the Mean Field Game theory to compute the deterministic user equilibrium, and Lebacque et al. (2022) computed the Stochastic User Equilibrium (SUE) for the generalized bathtub model. In this work, we deploy the latter modeling framework to capture the traffic dynamics and calculate the SUE.

1.2. Multimodality

Considering different transportation modes requires integrating different vehicle types into the road network. Multimodal macroscopic congestion models consider different travel times for the different vehicles and their interactions, especially between personal cars and buses. We can distinguish different approaches to represent multimodality in the literature: (i) the speeds for buses and cars are the same, and the bus dwell time is explicitly considered (Dakic et al., 2021); (ii) the bus speed is affine in the car speed (Loder et al., 2017, 2019); (iii) modes other than the private car undergo an additional delay depending on the congestion level (Loder et al., 2021); (iv) each mode has its speed function, which is affine in the accumulation of every mode in the system (Paipuri and Leclercq, 2020). In this work, we use the second approach to capture the impact of car congestion on PT without adding excessive complexity and calibration requirements.

Considering different vehicles may not be enough to account for the diversity of mobility supply, especially with the rise of ride-hailing and -sharing services. A passenger car offers two different transportation alternatives if driven alone or used for carpooling. Certain recent contributions in the literature (Xiao et al., 2016; Yu et al., 2019; Xiao et al., 2021b,a) have promoted carpooling to foster more sustainable travel behavior by reducing the number of vehicles in circulation. In the general framework, two travelers with similar trips would use only one car instead of two cars. On the one hand, users can drive on the High Occupancy Vehicle (HOV) lane, with the travelers sharing the expenses: fuel, congestion pricing, or credit/permit purchase. On the other hand, carpooling induces a penalty representing the detour, waiting time or the discomfort of not driving alone. The aim of this work is to integrate time-dependent TCS, congestion dynamics and multimodality, including carpooling, into a single framework.

1.3. TCS models in urban areas

A substantial part of the literature on TCS is aimed at optimizing travelers' route choices by charging the links of the networks, e.g., Yang and Wang (2011). The implementation of these contributions in an urban area is complex in practice. The present work focuses on mode and departure time choices at the network level. Most studies in the literature have used *Vickrey's bottleneck* model to address TCS at the network level to reduce congestion (Nie and Yin, 2013; Tian et al., 2013; Nie, 2015; Xiao et al., 2015; Jia et al., 2016; Miralinaghi et al., 2019). Furthermore, Bao et al. (2019) considered *Chu's model* (Chu, 1995), which is based on the BPR function. In the studies mentioned, the credit charge is dynamic, meaning the number of credits required to pass the bottleneck is time-dependent (i.e., based on the choice of departure time). The purpose is to encourage travelers to switch from on-peak to off-peak hours. However, most considered only a single transportation mode with a homogeneous traveler profile. Tian et al. (2013), Xiao et al. (2015) and Miralinaghi et al. (2019) accounted for different Values of Time (VoT) to represent the heterogeneity of monetary valuation of travel time for the personal car with Vickrey's bottleneck.

Balzer and Leclercq (2022) propose a TCS based on the trip-based MFD in order to capture trip heterogeneity (trip length) and congestion dynamics at a large scale. We considered Public Transportation (PT) with a fixed cost based on a given departure time

Table 1
Comparison of the different contributions on TCS.

Article	Congestion model			Travel choice				Different VoT	Dynamic charging scheme	Pollution
	Vickrey	Trip-based MFD	Multimodal generalized bathtub	Departure time	Car	PT	Carpool			
Nie and Yin (2013)	✓			✓	✓					
Tian et al. (2013)	✓			✓	✓	✓		✓	✓	
Nie (2015)	✓			✓	✓				✓	
Xiao et al. (2015)	✓			✓	✓			✓	✓	
Jia et al. (2016)	✓			✓	✓				✓	
Miralinaghi et al. (2019)	✓			✓	✓			✓	✓	
Bao et al. (2019)	✓			✓	✓				✓	
Liu et al. (2022)		✓		✓	✓			✓	✓	
Balzer and Leclercq (2022)		✓			✓	✓				✓
This work			✓	✓	✓	✓	✓	✓	✓	✓

and origin–destination locations. The credit charge was static, i.e., the number of credits required does not depend on the departure time, as the focus is the shift from personal cars to PT. Recently, Liu et al. (2022) also used trip-based MFD without PT, while the dynamic credit charge is designed in proportion to the travel distance. In this work, the TCS is dynamic and depends on the users' departure time and mode (private car, PT, and carpooling) choices. In addition, we consider a multimodal extension of the generalized bathtub model (Jin, 2020) to address the network equilibrium with a heterogeneous demand profile and investigate the effect of a TCS on mode and departure time choices.

Moreover, we take into account environmental measures (CO2 emissions) not only to evaluate the performance of TCS but also to optimize the dynamic charging profile. In the literature, few studies consider environmental goals with TCS at the link level (Gao and Sun, 2014). To highlight our contributions, we compare the most relevant studies on TCS at the network level, including the departure time choice problem in Table 1, along with previous works on MFD under TCS. This study addresses the gap between realistic congestion representation and dynamic TCS. It should be recalled that dynamic TCS means that the credit charge may change depending on the time. The time- and mode-dependent TCS is aimed at fostering shifts ofmode and departure times to mitigate congestion and reduce the carbon footprint of the transportation network. We consider three travel modes: personal car, PT, and carpooling.

The remainder of this paper is organized as follows. In Section 2, we present the multimodal generalized bathtub framework with the TCS: congestion dynamics, TCS, users' decision, and equilibrium formulation. Section 3 formulates the computation of the SUE and the optimization of the credit charge profile. The case study and the associated results are presented in Section 4 for a realistic morning commute scenario in Lyon (France) with 384,200 trips in total. Section 5 concludes this paper.

2. Problem formulation

This section describes the proposed methodological framework to address the TCS problem, including the SUE calculation based on the multimodal generalized bathtub under TCS. Fig. 1 depicts an overview of the different components and interactions in our framework. In Fig. 1, the travelers get a fixed amount of credits daily from the regulator. Obviously, this amount is insufficient to travel by car during peak hours. Otherwise, the TCS would not discourage solo car rides. Travelers can trade the credits on a specific market. They choose their transportation mode and departure time according to the credit charging profiles and scheduling preferences. The regulator determines the credit charging profile to achieve its economic and environmental goals. The related measures (e.g., total travel time and carbon emissions) depend on the travelers' behaviors. The credit price results from the supply and demand in this market, so it depends on the travelers' choices. Thus, there are complex interdependencies between travelers' choices, the market, and the traffic congestion level. While describing credit price evolution during the transitional phase is very challenging, it is possible to calculate the credit price at equilibrium when all interactions stabilize. The following subsection presents the congestion model based on the generalized bathtub. Then the TCS is presented with a dynamic charging profile. Finally, we present the user choice model and the SUE formulation.

For convenience, the notations are summed up in Table 2.

2.1. Multimodal generalized bathtub

Here we introduce the concepts, assumptions, and notations related to the congestion model.

In this framework (see Fig. 1), travelers have different characteristics: trip length $l \in \mathcal{L}$, desired arrival time, $t_a \in \mathcal{T}_a$, and scheduling preferences α_c, $\tilde{\beta}_c$, and $\tilde{\gamma}_c$ associated to their socioeconomic class $c \in \mathcal{C}$. The capital and curly letter represents the domain of validity of the respective parameter or variable. They choose their departure times $t_d \in \mathcal{T}_d$ and travel modes $m \in \mathcal{M}$ according to the corresponding travel costs. $\mathcal{M}$ is the discrete set of all available transportation modes.

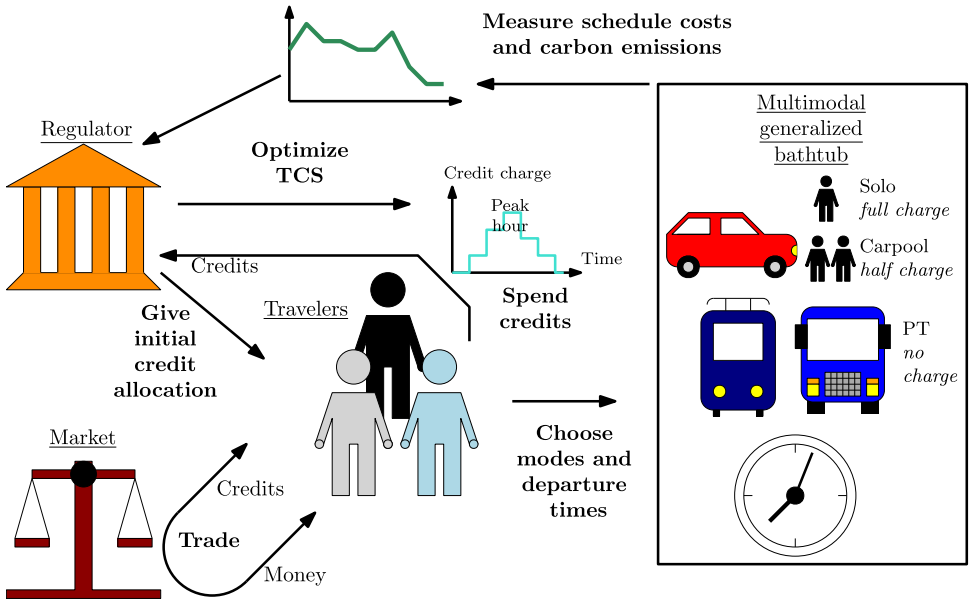

Fig. 1. Framework of the multimodal bathtub under TCS.

The demand scenario defines their VoT, trip length, and desired arrival time for all users. It is described by the distribution $d = d(c, l, t_a)$. D denotes the total number of travelers. Traffic assignment will allocate each user to a departure time and a mode. We represent the user distribution by the distribution f that encompasses all their characteristics (VoT, trip length, desired arrival time, departure time, mode) $f = f(c, l, t_a, t_d, m)$. In this paper, we consider three transportation modes: car solo (one traveler per car), carpooling (two travelers per car), and public transportation (PT). ζ_m is the waiting time linked to mode m. We set it to zero for the solo car drivers and PT riders. We neglect the PT waiting time (typically half of the head time) as we focus on the morning commute scenario when the PT frequency is high and the average waiting time is only a few minutes. It represents the extra time related to carpooling (waiting and small detour time) in this paper. We assume no distinction between driver's and passenger's travel time and credit charge when carpooling. It means the driver waits at its origin, and its waiting time in its car is equivalent to the passenger walking time to the driver's origin during ζ_m. Then both start their trips.

The user cost of mode m is calculated based on the arrival time obtained by bathtub dynamics equations. This congestion model assumes all trips take place in the same overall region, where the speed is spatially uniform. The mean speed for a given time is a function of the number of vehicles (personal cars, buses, tramways) circulating in the network at this time. A vehicle enters the network at the departure time t_d and leaves it once it has driven its trip length l. The generalized bathtub model provides a set of equations per transport mode. For each mode m, we define a virtual traveler $t \mapsto z_m(t)$ which keeps track of the cumulative traveled distance since the origin of times, as introduced by Lamotte and Geroliminis (2018) (a.k.a. characteristic travel distance in Jin, 2020). We also define $H_m(t)$ as the accumulation, i.e., the number of vehicles of type m in the network at time t. The number of active trips with a remaining distance higher than x at t is denoted $k_m(x, t)$. This state variable is specific to the generalized bathtub. The accumulation is then computed by $H_m(t) = k_m(x = 0, t)$. Recall that the accumulation is a state variable common to both MFD and bathtub representations. The speed of mode m v_m depends on the accumulations of all modes (Loder et al., 2017, 2019, 2021; Paipuri and Leclercq, 2020; Paipuri et al., 2021). The coupling between the modes in the bathtub model occurs through the speed functions.

The accumulation at time t consists of the trips that started before t and are long enough to be ongoing by t. Therefore, we introduce the density, with respect to departure time t_d, of the number of vehicles with trip length longer than l: $F_m(l, t_d)$. The traffic dynamics are based on the formulation of Ameli et al. (2022) and extended here to account for different modes. The bathtub dynamics of mode $m \in \mathcal{M}$ is given by Eq. (1).

$$\begin{cases} z_m(t) & = \int_0^t v_m(\{H_{m'}(s)\}_{m' \in \mathcal{M}}) \mathrm{d}s \\ H_m(t) & = \int_0^t F_m(z_m(t) - z_m(t_d), t_d) \mathrm{d}t_d \\ F_m(l, t_d) & = \int_{l' > l, l' \in \mathcal{L}} \int_{t_a \in \mathcal{T}_a} \sum_{c \in \mathcal{C}} f(c, l', t_a, t_d, m) \mathrm{d}l' \mathrm{d}t_a \end{cases} \tag{1}$$

The first equation states that the mean speed depends on the accumulations and computes the trajectory of the virtual traveler $z_m(t)$. The second computes the accumulation $H_m(t)$: the sum of the trips that started earlier and are long enough to remain active. It depends on the trajectory of the virtual traveler $z_m(t)$. The third equation is the computation of the density $F_m(l, t_d)$ based on the traffic assignment f. The natural setting for the solutions of Eq. (1) is the space of Lipschitz continuous functions of time. In this space, it can be shown that given a distribution f, the solution (z_m, H_m) of Eq. (1) exists, is unique and depends continuously on

Table 2
Summary of parameters and variables notations.

Notation	Meaning
Parameters	
Ω	Ensemble of travelers' characteristics and choices.
Ω_m^W	Subspace of Ω restricted to mode m and charging period W.
$\Omega_m^W\{l\}$	Ω_m^W further restricted to trips of length l.
C	Ensemble of travelers classes (VoT).
c	Traveler's class.
α_c	VoT of class c.
$\tilde{\beta}_c$	Normalized marginal early cost of class c.
$\tilde{\gamma}_c$	Normalized marginal late cost of class c.
$\mathcal{L}$	Ensemble of trip lengths.
l	Trip length.
$\mathcal{M}$	Admissible modes.
$\mathcal{T}_a$	Ensemble of desired arrival times.
t_a	Desired arrival time.
$\mathcal{T}_d$	Admissible departure times.
$d(c,l,t_a)$	Travel demand distribution for class c, trip length l, and desired arrival time t_a.
D	Total number of travelers.
χ_{opt}	Optimization parameter.
κ	Credit allocation.
$\tau(t_d,m)$	Credit charge for mode m starting at t_d.
T_{charges}	Duration of a charging period.
θ_c	Logit parameter of traveler class c.
ζ_m	Waiting time/penalty with mode m.
E^*_{CC}	Credit Cap error goal.
E^*_{MCC}	Market Clearing Condition error goal.
E^*_{SUE}	Stochastic User Equilibrium error goal.
Discretization parameters	
Δ_l	Trip length resolution.
Δ_t	Departure time resolution.
Δ_{t_a}	Desired arrival time resolution.
i_l	Trip length index.
i_t	Simulation time index.
i_{t_d}	Departure time index.
i_{t_a}	Desired arrival time index.
$l_{\min}$	Minimum trip length.
$t_{a,\min}$	Minimum desired arrival time.
Variables	
ψ	Logit decision.
μ	Assignment update coefficient.
ω	Traveler's characteristics and choices.
$f(c,l,t_a,t_d,m)$	User distribution for class c, trip length l, desired arrival time t_a, departure time t_d, and mode m.
$F_m(x,t)$	Number of active trips with remaining distance longer than x at t.
$H_m(t)$	Accumulation at time t for mode m.
m	Mode index.
p	Credit price.
$\hat{t}_a$	Arrival time.
t_d	Departure time.
v_m	Instantaneous speed of mode m.
$z_m(t)$	Virtual traveler traveled distance at time t with mode m.
TT	Travel time.
TC	Travel cost.
UC	User cost.
r	Search index for SUE.
R	Normalized credit consumption excess.
E_{CC}	CC error.
E_{MCC}	MCC error.
E_{SUE}	SUE error.
$\mathcal{F}$	Travel characteristics to be updated.
$\bar{\mathcal{F}}$	Travel characteristics not to be updated.
W	Charging period index.
Obj_W	Objective function for charging period W.
ΔObj_W	Variation of the objective function for charging period W.
Γ	Travel cost gain.

f for the weak topology of bounded measures. This follows by adapting propositions 1 to 4, and their proofs (appendices B to E) in Ameli et al. (2022).

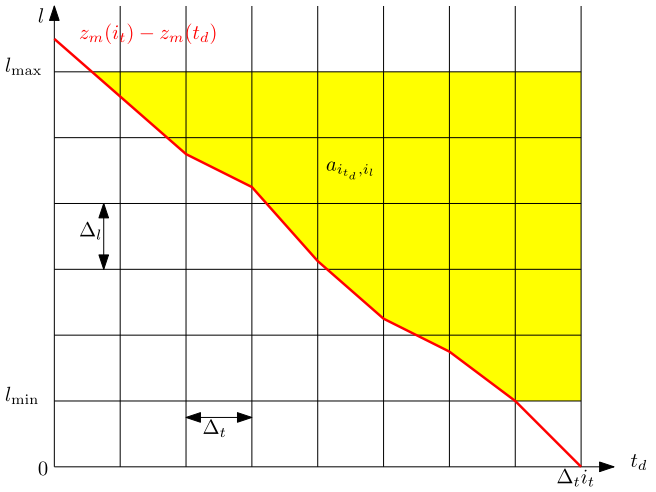

Fig. 2. Discretization of the accumulation computation.

The arrival time $\hat{t}_a$ is computed by using the inverse of the virtual traveler $x \mapsto z_m^{-1}(x)$. The inverse is correctly defined as long as the mode speeds are always non-zero. We assume the mean speeds are always strictly positive, meaning we exclude the possibility of a complete gridlock. A user starting at t_d with a trip of length l and using mode m will arrive at

$$\hat{t}_a = t_d + z_m^{-1}(z_m(t_d) + l) + \zeta_m. \tag{2}$$

If the mode speeds are bounded from below, it can be shown that $\hat{t}_a$ depends continuously on (l, t_d) and that the function $(l, t_d) \mapsto \hat{t}_a$ depends continuously on f for the weak topology of bounded measures. This result follows by adapting proposition 5 and its proof (appendix G) in Ameli et al. (2022). To address the realistic demand profile based on trip data, we use the discretization approach to represent the formulation of the multimodal generalized bathtub to compute the arrival times via the trajectory of the virtual traveler z_m and the accumulation H_m, which are inter-dependent.

Discretization

The discretization approach aims to compute the arrival times of the multimodal generalized bathtub (Eq. (1)) in uniform intervals. Note that the discretization is not applied in our previous study, Balzer and Leclercq (2022), since we used a more advanced trip-based MFD simulation framework, wherein the arrival times are computed following an event-based simulation: the state variables are updated each time a vehicle enters or leaves the network. The equilibrium computation was based on the linearization of the travel times with respect to the mode choices. This former approach is not suited here for the following reasons: (i) the travel time linearization while accounting for departure time becomes too complex as it adds another dimension to the problem; (ii) for each trip length, departure time, and mode, we would need one agent to account for the effect of this specific demand on the congestion. The computational cost of event-based resolution of the trip-based MFD increases quickly with the number of agents, as the state variables are updated each time an agent enters or leaves the network. The main difference between the two approaches is that the trip-based MFD framework follows each traveler and tracks its remaining travel distance. On the contrary, the generalized bathtub focuses on the distribution of the remaining trip lengths with fixed time steps. It is advantageous in terms of complexity and computation time to use the generalized bathtub framework, which is continuous. However, in a later Section 4.3, we will simulate the optimal TCS solution with the more advanced trip-based MFD formulation to show that using the simplified approximation through the discretization of the generalized bathtub model in the optimization process makes perfect sense.

Details of the discretization are presented in Appendix A.

The dynamics computation involves the resolution of Eq. (1) time step after step. The integration of the virtual traveler trajectory is straightforward: on each time step i_t, the traveled length z_m increased with the speed corresponding to the previous accumulation $H_m(i_{t-1})$ plus the trips starting in this step. The accumulation computation is represented by the yellow area in Fig. 2.

The accumulation at the time $t = \Delta_t i_t$ gathers all vehicles that have already started their trips and have a remaining travel distance strictly positive. Each square contributes to the accumulation at i_t with $a_{i_{t_d},i_l} \in [0, 1]$ the ratio of the square above the line $t_d \mapsto z_m(i_t) - z_m(t_d)$ (i.e., the yellow part) multiplied by the number of trips starting at i_{t_d} with trip length i_l, $\sum_{c,i_{t_a}} f(c, i_l, i_{t_a}, i_{t_d}, m)$.

2.2. Dynamic tradable credit scheme

After presenting how traffic dynamics are affected by travelers' choices, we introduce the proposed demand management policy designed for the regulator to incite travelers to change their behaviors. Some mobility alternatives require credits depending on

the transportation mode m and departure time t_d. The credit charge is significant for highly congestive modes like private cars during peak hours and low for more sustainable choices like PT or carpooling outside peak hours. The regulator should set the charging profile $\tau(t_d, m)$ according to congestion and carbon emissions goals. In the following, the regulator only chooses the profile for car drivers $\tau(t_d, \text{car})$. It is free for PT riders: $\tau(t_d, \text{PT}) = 0$ and only the half for carpoolers as we assume two travelers per car: $\tau(t_d, \text{pool}) = \frac{1}{2}\tau(t_d, \text{car})$. Travelers receive a free initial allocation of κ credits from the regulator. They can trade the credits between themselves in a dedicated market. The credit price p is not fixed by the regulator. This is the main difference with congestion pricing: with TCS, the regulator defines the quantity and not the price, while for pricing, the regulator sets up the price but not the quantity. When equilibrium is reached, TCS and pricing may lead to the same results, but TCS makes it easier to meet collective optimum as the quantity is defined by design. It is determined by the law of supply and demand in the market. We do not consider the details of the trade mechanism. We adopt the widely used Market Clearing Condition (MCC), as in Yang and Wang (2011), to represent the market mechanism: the price is zero or all issued credits are spent.

2.3. Mode and departure time choice

Travelers' choices depend on the travel times depending on the traffic dynamics, the different alternatives, and the additional cost caused by the TCS, depending on the credit charge and the credit price. The travel time (TT) of a traveler leaving at t_d and arriving at $\hat{t}_a$ is

$$TT = \hat{t}_a - t_d. \tag{3}$$

The travel cost (TC) accounts for the early or late arrival on top of the TT. The TC of a traveler of the class c with the desired arrival time t_a finishing its trip at $\hat{t}_a$ is

$$TC = \alpha_c \left((\hat{t}_a - t_d) + \tilde{\beta}_c \max(0, t_a - \hat{t}_a) + \tilde{\gamma}_c \max(0, \hat{t}_a - t_a) \right). \tag{4}$$

$\alpha_c, \tilde{\beta}_c$, and $\tilde{\gamma}_c$ are respectively the VoT (money per time) and the normalized marginal cost (no unit) for early and late arrival.

The user cost (UC) is obtained by adding the TCS-related cost, i.e., the monetary value of the required credits:

$$UC = TC + p \cdot \tau(t_d, m). \tag{5}$$

Both TC and UC depend on trip length, departure time, mode, desired arrival time, and class. However, we do not make it explicit in the equations to keep the notations light.

We assume the users' decision processes follow the logit model to account for irrationality and uncertainty in their choices while keeping the framework tractable. The discrete logit-based decision depends on the UC of all alternatives regarding departure time and mode choice and on the logit parameter θ_c:

$$\psi(c, i_l, i_{t_a}, i_{t_d}, m) = \frac{e^{-\theta_c UC(c, i_l, i_{t_a}, i_{t_d}, m)}}{\sum_{i_{t'_d}, m'} e^{-\theta_c UC(c, i_l, i_{t_a}, i_{t'_d}, m')}}. \tag{6}$$

$\psi(c, i_l, i_{t_a}, i_{t_d}, m)$ is the ratio of travelers with characteristics c, i_l, i_{t_a} *wanting* to travel at t_d with mode m. It may be different from the *actual* travel choices $f(c, i_l, i_{t_a}, i_{t_d}, m)/d(c, i_l, i_{t_a})$. We assume all travelers have access to all modes. We especially consider all travelers have access to a car: the one they own, if they own one, or a shared or rental car. Such an assumption can also be found in Tian et al. (2013) and Xiao et al. (2021b).

2.4. Equilibrium formulation

The SUE formulation is based on Lebacque et al. (2022). It is extended to account for the mode choice and the TCS constraints. The SUE is reached when the user distribution matches the logit distribution:

$$d(\omega)\psi(\omega) = f(\omega) \ \forall \ \omega \in \Omega, \tag{7}$$

with $\Omega = \mathcal{C} \times \mathcal{L} \times \mathcal{T}_a \times \mathcal{T}_d \times \mathcal{M}$ the space of all travelers' characteristics and degrees of freedom. The demand conservation requires the travel demand with specific characteristics to match the sum of the user distributions with the same characteristics:

$$\sum_{i_{t_d}, m} f(c, i_l, i_{t_a}, i_{t_d}, m) = d(c, i_l, i_{t_a}) \ \forall \ c, i_l, i_{t_a}. \tag{8}$$

The TCS-specific constraints are, respectively, the credit cap (CC): the consumed credits cannot exceed the allocated amount, the MCC, and the positivity of the price:

$$\begin{cases} \sum_{\omega \in \Omega} f(\omega)\tau(\omega) \leq D\kappa; \\ \left(\sum_{\omega \in \Omega} f(\omega)\tau(\omega) - D\kappa \right) p = 0; \\ p \geq 0. \end{cases} \tag{9}$$

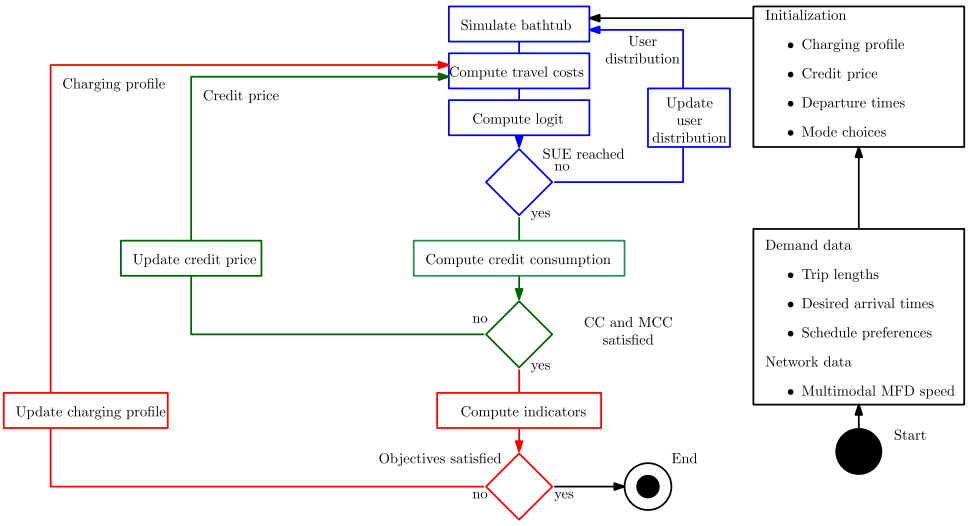

Fig. 3. Algorithm flowchart.

3. Methodological framework

Our contribution consists in computing the SUE under TCS, i.e., finding the travelers' choices (mode and departure time) and the credit price; and optimizing the credit charge τ to fulfill societal goals in terms of total travel cost and carbon emissions. Previous works on the generalized bathtub (Ameli et al., 2022; Lebacque et al., 2022) focused on calculating departure time distribution, excluding mode choice and optimization of TCS variables, i.e., a part of the blue inner loop. The equilibration of the multimodal generalized bathtub model under TCS is decomposed into two imbricated loops. The outer loop increases (respectively decreases) the price if too many (too few) credits are consumed until the MCC and CC hold: (i) price is zero and some credits are not used, or (ii) all credits are consumed. The inner loop changes the travelers' departure times and travel modes until their logit-based decisions match their actual travel choices. The two loops form two imbricated fixed-part problems to be solved. Fig. 3 presents the two loops: blue for the assignment and green for the credit price. The red one indicates the optimization of the charging profile. It is not part of the fixed-point problem. The role of this third loop is presented in Section 3.3.

3.1. Credit price

We define the credit consumption excess R as

$$R = \frac{1}{D} \sum_{\omega \in \Omega} f(\omega) \left(\frac{\tau(\omega)}{\kappa} - 1 \right). \tag{10}$$

It is the normalized number of credits used minus the initial allocation. The CC dictates it should be negative: we accept unused credits but not the consumption of non-existing ones. The CC error is defined as the positive part of R:

$$E_{\text{CC}} = \max(0, R). \tag{11}$$

The MCC error is defined as

$$E_{\text{MCC}} = p\kappa|R|. \tag{12}$$

It is high when the price is non-zero, and all credits are not consumed. We use the absolute value of R to ensure a positive metric for the MCC error.

We change the credit price if one of the error measures E_{CC} or E_{MCC} is higher than the given respective thresholds E^*_{CC} and E^*_{MCC}. The price variation of the CC and MCC loop for the iteration $i_{\text{step,pri}}$ of the price loop is

$$\Delta p = \frac{1}{\sqrt{i_{\text{step,pri}}}} \frac{1}{\kappa} R. \tag{13}$$

The amplitude of the change decreases as the loop iterates to force convergence but not too fast to allow for space exploration. This process is typical when solving a fixed-point problem, e.g., the Method of Successive Average (MSA) (Sheffi, 1985). We bound Δp by $\pm\epsilon_p$, a fixed threshold, to prevent large oscillations. The price is then updated by ensuring it stays positive:

$$p = \max(p + \Delta p, 0). \tag{14}$$

The price loop iterates until the maximum number of iterations is reached or both CC and MCC errors fall below the given thresholds.

3.2. Assignment

The SUE error quantifies the difference between user distribution and logit-based decision:

$$E_{\text{SUE}} = \frac{1}{D} \sum_{\omega \in \Omega} |f(\omega) - d(\omega)\psi(\omega)|. \tag{15}$$

The assignment loop starts with an initial solution based on free flow mean speed and then iterates until the maximum number of iterations is reached or the SUE error falls below a threshold E^*_{SUE}. A heuristic reassignment algorithm is designed to correct the worst decisions (assignment far from logit) with a procedure similar to the MSA. We first rank the assignment based on the SUE error. Then, we choose the proportion of the assignments with larger errors and reassign their departure time and mode choice. This procedure is inspired by Sbayti et al. (2007). The proportion corresponds to the step size of the algorithm. A search index is defined and initialized with $r = 1$. For each iteration of the SUE loop, the fraction $1/r$ of the assignment characteristics $\omega \in \Omega$ where the assignment error $|f(\omega)/d(\omega) - \psi(\omega)|$ is the largest, is updated. We name this part of the travel characteristics $\mathcal{F}$. The rest of the characteristics define the ensemble $\bar{\mathcal{F}}$. Thus $\mathcal{F} \cup \bar{\mathcal{F}} = \Omega$ and $\mathcal{F} \cap \bar{\mathcal{F}} = \emptyset$. The step size formulation is the same as the step size of the MSA method; however, we use the smart step size approach (Ameli et al., 2020) to update the step size for the following iterations. If the new user distribution leads to a smaller SUE error E_{SUE}, then the search index stays the same. Otherwise, the search index r increases by one, decreasing the search radius. The convergence of this approach is discussed in Ameli (2019). We stop once the SUE error falls below a given threshold or the best solution (lowest SUE error) is returned if the maximum number of iterations is reached. The implementation of the algorithm for SUE calculation is detailed in Appendix B.

3.3. Optimization of the charging profile

The charging profile is updated using an iterative heuristic method to decrease congestion and pollution. We estimate the variation of the travel costs and the carbon emissions for a change in car share for each charging period W of duration T_{charges} (typically half an hour). An alternative method for credit profile optimization could have been Bayesian optimization as in Liu et al. (2022). As we could derive an analytical approximation for the gradient considering the system dynamics, we better stick to the proposed heuristic that converges quickly with reasonable accuracy. Fig. 4 presents the updating process. We do not account for the change of early and late penalties but only consider the travel time variation to have a robust measure. We do not consider carpooling in this approximation, as the corresponding share is relatively small. Let us define Ω^W_m the subspace of Ω restricted to mode m and departure time included in the charging period W, i.e., $\Omega^W_m = C \times \mathcal{L} \times \mathcal{T}_a \times (\mathcal{T}_d \cap W) \times \{m\}$. $\Omega^W_m\{l\}$ is the subpart further restricted to trips of length l, i.e., $\Omega^W_m\{l\} = C \times \{l\} \times \mathcal{T}_a \times (\mathcal{T}_d \cap W) \times \{m\}$. We define several aggregates over this period W for each mode m:

- the average speed $\bar{v}_m = \frac{\sum_{t \in W} H_m(t) v_m(t)}{\sum_{t \in W} H_m(t)}$;
- the average travel cost $\bar{TC}_m = \frac{\sum_{\omega \in \Omega^W_m} f(\omega) TC(\omega)}{\sum_{\omega \in \Omega^W_m} f(\omega)}$;
- the average travel time $\bar{TT}_m = \frac{\sum_{\omega \in \Omega^W_m} f(\omega) TT(\omega)}{\sum_{\omega \in \Omega^W_m} f(\omega)}$;
- the average trip length $\bar{l}_m = \sum_{l \in \mathcal{L}} \frac{\sum_{\omega \in \Omega^W_m\{l\}} f(\omega) l}{\sum_{\omega \in \Omega^W_m\{l\}} f(\omega)}$.

The ratio between the average accumulation $\frac{\sum_{t \in W} H_m(t) \Delta_t}{T_{\text{charges}}}$ and the number of travelers $\sum_{\omega \in \Omega^W_m} f(\omega)$ is named $\tilde{H}_m$. It is approximated using the travel times: $\tilde{H}_m = \bar{TT}_m / T_{\text{charges}}$. We now compute the effect of a traveler switching from car to PT, i.e., when $\sum_{\omega \in \Omega^W_{\text{car}}} f(\omega)$ decreases by one. It corresponds to a reduction of the mean car accumulation by $\tilde{H}_{\text{car}}$. A decrease in car ridership affects the average TC of all modes by increasing the mean speeds. This variation is approximated by

$$\delta_v \bar{TC}_m = -\frac{\mathrm{d}\bar{\alpha} \frac{\bar{l}_m}{\bar{v}_m}}{\mathrm{d} \sum_{\omega \in \Omega^W_{\text{car}}\{l\}} f(\omega)} = \bar{\alpha} \frac{\mathrm{d}v}{\mathrm{d}H_m} \tilde{H}_m \frac{\bar{l}_m}{\bar{v}^2_m}. \tag{16}$$

$\bar{\alpha}$ is the average VoT. The variation of total travel cost is approximated by $\sum_{\omega \in \Omega^W_m} f(\omega) \delta_v \bar{TC}_m$

The marginal total travel cost variation ΔTC_{tot} due to a decrease in car ridership, i.e., because a user switches from car to PT, is the change of travel cost for this user plus the effect on the rest of the travelers:

$$\Delta TC_{\text{tot}} = \bar{TC}_{\text{PT}} - \bar{TC}_{\text{car}} + \sum_m \sum_{\omega \in \Omega^W_m} f(\omega) \delta_v \bar{TC}_m. \tag{17}$$

The carbon emission per distance e depends on the mean network speed. We use the COPERT IV (Ntziachristos et al., 2009) model of Lejri et al. (2018). It allows for efficient estimation of the pollution while accounting for the effect of the congestion dynamics through the variations of the mean car speed across time. We only consider private car carbon emissions, but the model can easily be tuned to account for different fleet compositions. We do not account for the variation of PT carbon emissions due to occupancy (more weight) or operational (more vehicles) changes. Indeed, a large part of the PT fleet uses low-carbon technologies: electric propulsion for subways, tramways, and some buses; and natural gas for some other buses. The change in PT carbon emissions is thus neglected. We approximate the carbon emissions by using the mean car speed over the charging window $e(\bar{v}_{\text{car}})$. The total distance

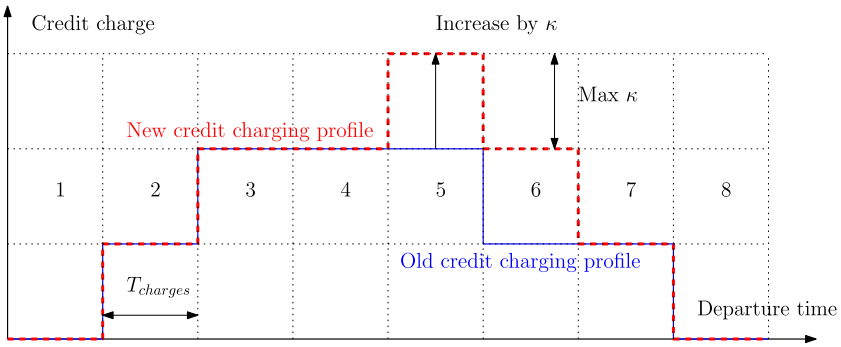

Fig. 4. Update of the credit charging profile from blue to red.

driven by car is $l_{\text{tot}} = \sum_{l \in \mathcal{L}} l \sum_{\omega \in \Omega^W_{\text{car}}\{l\}} f(\omega)$. The marginal carbon emission decreases when a traveler switches to PT consists of the emission of a car $e(\bar{v}_{\text{car}})\bar{l}$ and the effect of better traffic conditions $l_{\text{tot}} \frac{\mathrm{d}e}{\mathrm{d}\sum_{\omega \in \Omega^W_{\text{car}}} f(\omega)}$.

$$\Delta E = -e(\bar{v}_{\text{car}})\bar{l} - l_{\text{tot}} \frac{\mathrm{d}e}{\mathrm{d}\sum_{\omega \in \Omega^W_{\text{car}}} f(\omega)} = -e(\bar{v}_{\text{car}})\bar{l} - l_{\text{tot}} \frac{\mathrm{d}e}{\mathrm{d}v_{\text{car}}}(\bar{v}_{\text{car}}) \frac{\mathrm{d}v_{\text{car}}}{\mathrm{d}H_{\text{car}}} \tilde{H}_{\text{car}} \tag{18}$$

The global objective function Obj_W to minimize over the charging period W is a combination of the total travel cost TC_{tot} and carbon emissions E. It is defined by

$$Obj_W = TC_{\text{tot}} + \chi_{\text{opt}} E, \tag{19}$$

with χ_{opt} the optimization parameter chosen to tune the relative importance of pollution compared to congestion. Its variations in reaction to a credit charge increase, i.e., a decrease in car ridership, is

$$\Delta Obj_W = \Delta TC_{\text{tot}} + \chi_{\text{opt}} \Delta E. \tag{20}$$

The variation of the objective function ΔObj_W is computed for each charging period. The credit charge of the period with the highest absolute variation is updated: it increases if negative and decreases if positive. The other charging periods are changed only if the difference between two consecutive periods is too high. In our case study, the credit charge of the concerned period is updated by one allocation κ. We allow a maximum difference of one allocation κ between consecutive periods. If needed, the other charging periods are updated to fulfill this requirement. This constraint limits the effect of travelers waiting for the change of period to start their trip and leading to a travel peak just at the period change. This process of 'braking' to avoid a high toll is presented in Lindsey et al. (2012). We provide the pseudo-code in Appendix C along a small example in Fig. 4. Period 5 is chosen to be updated (highest absolute gradient) by increasing the charge by κ. The charge in period 6 is increased to have no credit charge difference of more than κ.

The SUE is then computed with the new TCS profile, the estimation of the gradient of the objective function for the new equilibrium is estimated, and the credit profile is updated again. The optimization ends if a loop is detected, meaning we reached a charging profile that has already been considered or if the maximum number of iterations is reached.

4. Case study

The city of Lyon, France, serves as the framework for deriving travelers' choices and credit prices at equilibrium, along with optimizing the dynamic credit charge to minimize total travel time and carbon emissions. In the following, we introduce the case study. The effects of TCS, both at the global and individual scale, are then presented. Finally, the trip-based MFD cross-validates the results by providing a finer resolution of the traffic dynamics.

4.1. Simulation settings

The travel demand considered for the case study represents the typical morning commute of 384,200 travelers in Lyon (France) between 7:00 and 10:00. There are ten regions and five boundaries, creating 224 different OD-pairs with non-zero demand. The travel demand consists of trips in Lyon and through Lyon, i.e., we also account for travelers starting or/and ending their trip outside the city. Fig. 5(a) represents the network studied. The synthetic desired arrival times are shown in Fig. 5(b). The distribution has a bell shape: the demand is low at 7:00 and 10:00 and high between 8:00 and 9:00. The trip lengths range from 1.4 km to 16.3 km, as shown in Fig. 5(c).

An MFD speed function represents the network capacity. All trips occur in the same region. The mean speed depends only on the car accumulation (solo drivers and carpoolers). We assume the number of operating buses is given and thus already accounted for

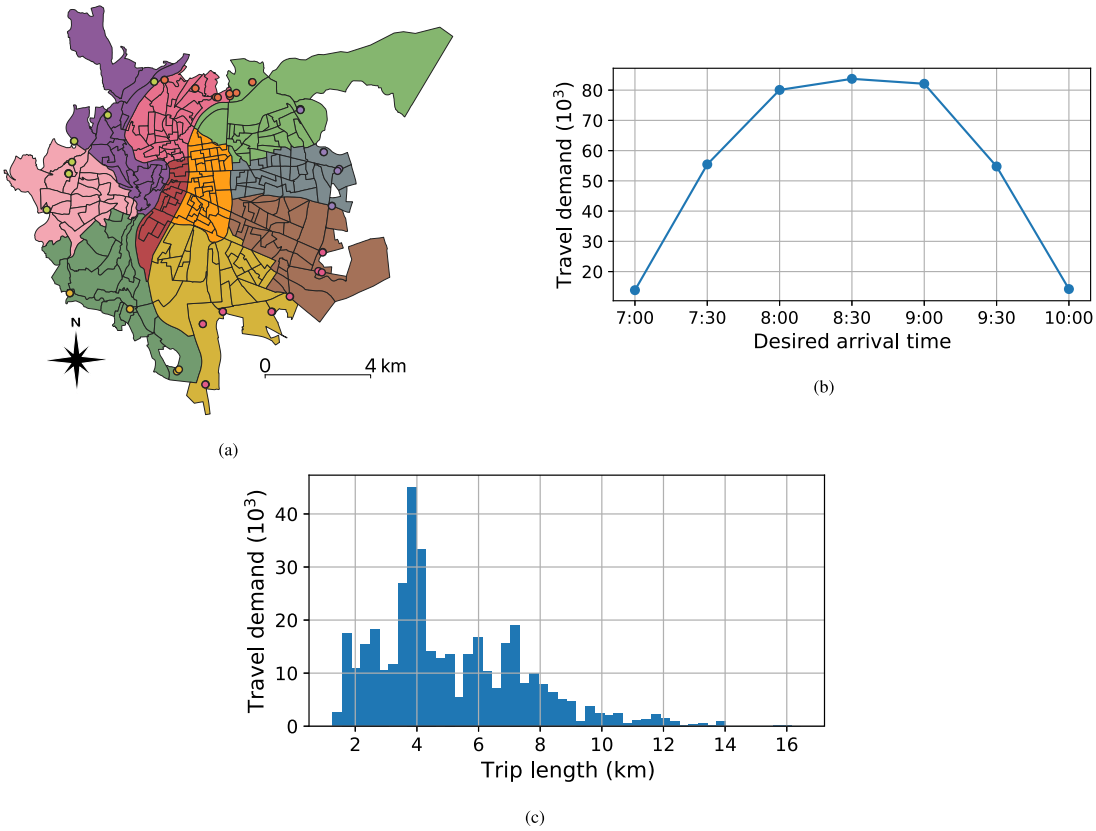

Fig. 5. Supply and demand for the scenario: (a) the ten regions formed by the IRIS areas and the access points merged in five boundaries (circles), (b) the distribution of the desired arrival times, and (c) the distribution of the trip lengths.

in the speed function. The speed function does not depend explicitly on the accumulation of buses. Instead of taking PT travel times independently from the car accumulation, we calibrated the affine dependence formulation from Loder et al. (2017) with the travel times and distances retrieved from the city navigator (HERE Developer, 2020). The travel demand acts as the weighting factor. The PT speed is assumed affine in the car speed. As the PT trips may consist of different modes (subway, tramway, and bus), we obtain a macroscopic calibration of the PT speed, regardless of the PT vehicles. It is computed by (numerical values for speed in m/s):

$$V_{\mathrm{PT}} = 0.12 V_{\mathrm{car}} \left(H_{\mathrm{car}} + \frac{1}{2} H_{\mathrm{pool}} \right) + 3.17. \tag{21}$$

Note that the constant factor is higher and the proportionality factor lower than in Loder et al. (2017). In the former study, the authors represented the speed of buses only, whereas we consider tramways and subways as well. These modes are not or very little impacted by congestion. A mean car speed of 50 km/h leads to a mean PT speed of 17.4 km/h. For comparison, a similar car speed with Loder's models leads to a PT speed of 15.4 km/h for the center of Zurich and 20.6 km/h for the neighborhood of Wiedikon.

The trip length is discretized with 50 steps, and the departure time with 100 steps. We validate these choices in 4.3. We assume seven possible desired arrival times: every 30 min from 7:00 to 10:00. These numerical values are chosen as a trade-off between computation times, numerical rounding errors, and simulation precision. To account for the equity of the TCS concerning the travelers' wealth, we consider travelers with a low VoT of 10.8 EUR/h for low revenue and a high VoT of 21.6 EUR/h to represent high revenue. We assume they are evenly distributed across the travel demand. These VoT correspond to the order of magnitude of the VoT distribution of Lyon's inhabitants, as used in Ameli et al. (2021). The normalized early factor is chosen as 1/2 and the late one as 2. This means that being late is worse than traveling a long time, which is worse than arriving early. It is a common assumption when computing the travel cost as a proxy for the perceived user cost. The normalized ratios are similar to Arnott et al. (1990). This choice of discretization leads to 210,000 different combinations of travelers' characteristics and trip choices: 50 trip lengths, 100 departure times, seven desired arrival times, two VoT, and three modes.

The trip-based MFD provides the exact travel times by solving the implicit equation $l_m = \int_{t_d}^{\hat{t}_a} V_m(s)\mathrm{d}s$. It serves as our plant in this case study. The two main differences between the trip-based model and the generalized bathtub are: (i) trip lengths and desired arrival times which are individually assigned to each traveler in the trip-based model while being represented by distributions in the generalized bathtub; and (ii) the generalized bathtub uses discretization with arbitrarily fixed steps, whereas the trip-based MFD is solved following an event-based discretization (starts and ends of trips). The trip-based MFD (event-based resolution) solution

Table 3
The parameters used for the simulation.

Parameter	Notation	Value
VoT	α_c	{10.8, 21.6} EUR/h
Scaled early factor	$\tilde{\beta}$	1/2
Scaled late factor	$\tilde{\gamma}$	2
Endowment	κ	1 credit
SUE goal	E^*_{SUE}	10^{-2}
CC goal	E^*_{CC}	5×10^{-3}
MCC goal	E^*_{MCC}	5×10^{-3}
Maximum price variation	ϵ_p	1 EUR
Logit parameter	θ_c	1 1/EUR
Optimization parameter	χ_{opt}	{0, 10^{-4}, 10^{-3}}
Carpooling penalty	ζ_{pool}	10 min
Charging period	T_{charges}	30 min

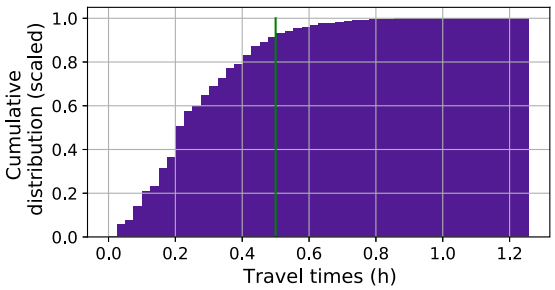

Fig. 6. Travel time distribution (without TCS). The charging period T_{charges} (30 min) is represented by the green line.

is expensive to compute for such a large set of trips. The trip-based framework updates the state variable each time a trip begins or ends, i.e., up to thirty thousand times (twice per agent and one agent per trip length, departure time, and mode). With the generalized bathtub, we count less than 200 time steps for the generalized bathtub (the departure times plus additional time steps to wait for the completion of the last trip). One simulation lasts about 470 s with the trip-based MFD and only 0.1 s with the generalized bathtub. The trip-based framework is used only to confirm that the generalized bathtub approximation provides a close approximation of the system states for the optimal solution.

We estimate the carpooling penalty ζ_{pool} with an additional 10 min. The sensitivity of this parameter is discussed in Appendix D. The main parameters used for the numerical computation are gathered in Table 3. Note that the endowment value κ is only meaningful when compared to the charging profile τ, as only the ratio matters.

The charging period is chosen based on the travel time distribution without TCS, in Fig. 6. The credit charge changes every 30 min, and most trips (about 90%) last less than this period. This means most of the trips finish at most in the period after which they started. It is essential not to have too many trips impacting many periods, as these travelers would impact the traffic conditions without paying the appropriate charge. This is in line with marginal cost pricing: the traveler pays for the externality they cause to the rest of the travelers.

We assess the convergence quality as a verification. The SUE loop is run until the SUE error falls below the given threshold E^*_{SUE}, i.e., when the user distribution is close enough to the logit decisions. The resulting assignment for an optimized TCS (referred to as 'mid' later in the text) is shown in Fig. 7 versus the demand weighted by the logit-based decision. Most of the points in Fig. 7(a) are on the diagonal, meaning the assignment matches the logit. Some points deviate, but as the error distribution shows (Fig. 7(b)), their number is low, and the error is small (max 12% for one point), thus the impact is marginal.

4.2. TCS impact analysis

We first assess the global effects of optimized TCS on the network: total travel cost, carbon emissions, credit charge, assignment changes. The aim of the algorithm proposed and presented in 3.3 is to minimize carbon emissions and the total travel cost. The total travel cost is the sum of all travelers the travel costs, i.e., the proxy for the economic losses caused by congestion. Different coefficients define the objective function to vary the importance of minimizing carbon emissions: 0, 10^{-4}, and 10^{-3}. We keep the solutions forming the Pareto front, i.e., those with no other solution being better simultaneously for the total travel cost and carbon emission reduction. As a benchmark, we also compute the equilibrium under static credit charging, with different charge over allocation ratios $\tau(\text{car})/\kappa$ between 3 and 16. The Pareto front is shown in Fig. 8, with the static solutions and the no TCS case for comparison. A static charge of 4 credits means that, on average, only one car can drive for every four travelers (one solo driver or two carpoolers). It already enables a reduction of the the total travel cost of about 19% and a 59% reduction of pollution. Dynamic charging profiles improve those metrics even further: 20% for congestion and 90% for pollution. It is possible to reach

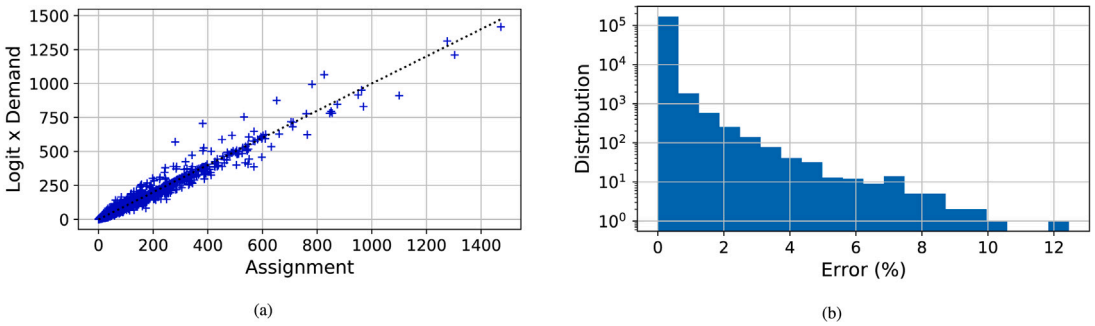

Fig. 7. Quality of the SUE: (a) user distribution vs. demand weighted by the logit, and (b) distribution of the relative error between the logit and user distribution over demand.

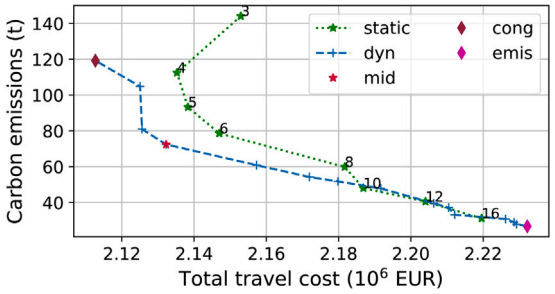

Fig. 8. Total travel cost vs. carbon emissions for different static and dynamic TCS. The numbers are the charge over allocation ratios for the static cases. For comparison, the no TCS case leads to a total travel cost of 2.63×10^6EUR and a carbon emission of 275 t.

similar pollution levels with static charging, as it decreases when the charge increases (fewer car drivers). However, it is achieved at the expense of the total travel cost reduction. To achieve a low carbon footprint, the TCS significantly penalizes the car, and many travelers switch to PT and carpooling. Since the mode shift is significant, the improvement of traffic does not offset the use of slower modes, and the total travel cost increases due to increased travel times. The total travel cost reduction of 20% (dynamic charging 'cong') cannot be reached with static charging. Although static charging enables a the total travel cost reduction of 19%, the associated carbon emissions are 36% higher than the dynamic TCS 'cong'. We keep the dynamic solutions with the lowest total travel cost ('cong') and the lowest CO2 emission ('emis') for further comparison against static charging. An intermediate case of dynamic charging ('mid') is compared versus the no TCS scenario. See Appendix E for comparing the TCS in terms of total travel time and carbon emissions.

The static and dynamic credit charge and equivalent toll profiles are presented in Fig. 9. We plot the charge for solo car drivers. It is half for carpoolers and zero for transit riders. The equivalent toll charge is defined as $(\tau(t_d, \text{car}) - \kappa)p$. It corresponds to the out-of-pocket money a traveler needs to pay to start a solo car trip at t_d. As expected, it is more expensive to drive a car during the high-demand period of the peak hour. Increasing the magnitude of carbon emissions increases the credit charge (Fig. 9(a)) as pollution tends to increase with car usage: the 'emis' scheme leads to an equivalent toll (Fig. 9(b)) of about 8 EUR, while it stays below 4 EUR in the 'cong' case.

We compare the modal shares for the different scenarios in Fig. 10. As expected, we see in Fig. 10(a) that the share of solo drivers diminishes with TCS as the associated user costs increase. On closer inspection it can be seen that the car share decreases with dynamic charging during the peak demand, while it increases with static charging. This can be explained by two effects: it becomes expensive to take the car as the credit charge is high during the peak in the dynamic case. The credit charge is the same in the static case, but the travel demand is higher. The TCS 'cong' strongly reduces the car share for a limited time (8:00 to 9:00), while the TCS 'emis' creates a substantial reduction across the whole time frame to reach ambitious pollution targets. The PT share (Fig. 10(b)) increases with the charging profile as it requires no credits. The share of carpoolers is captured in Fig. 10(c). The carpooling mode is used more with TCS than without TCS. However, the carpooling share decreases with the charging profile when the credit charge is high, as a carpooler still needs to spend credits. When looking at the shares with respect to the charging slots for all modes in Fig. 10(d), the TCS seems to make travelers leave later. The traffic conditions are improved, the travel times decrease, and thus travelers start their trip later to arrive around their desired arrival time. There is, however, very little difference between the different TCS. The conclusion is that the TCS affects the mode choice more than the departure time distribution. This is partly due to the limitation of the maximum difference of one allocation κ between two consecutive charging periods. The gain of shifting one's departure time for a charging period with a lower credit charge does not exceed the early/late arrival penalty.

In Fig. 11, the traffic conditions with and without TCS are compared through the mean speeds. Without TCS, the mean speeds of PT and cars (represented in Fig. 11(a)) are similar during the peak demand. Although the equilibrium is not deterministic, the user

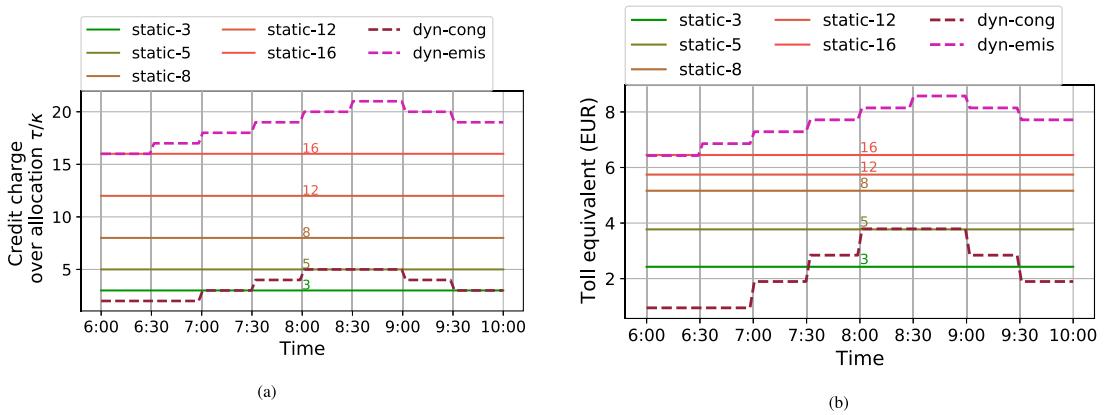

Fig. 9. Comparison of the static and dynamic TCS for different parameters: (a) credit charge and (b) toll equivalent with respect to the departure time slots.

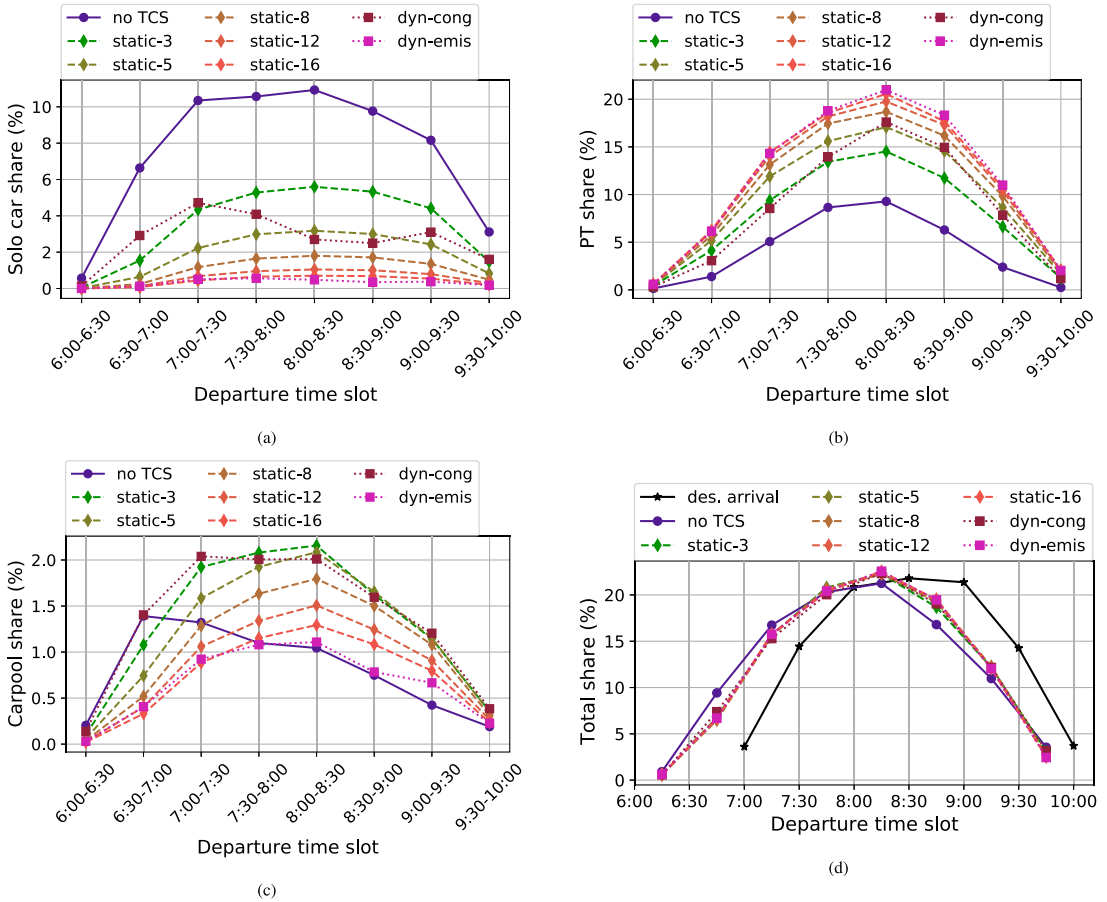

Fig. 10. Evolution of the mode shares and the departure times for (a) solo car, (b) PT, (c) carpool, and (d) total shares.

costs are similar, as both modes are used. As expected, the TCS improves traffic conditions by reducing the number of circulating cars. The gain is considerable for cars, which circulate about 20 km/h faster during the peak period. The PT speed increases by about 4 km/h. The waves come from the discretization of the desired arrival times. This leads to several local demand peaks every half hour. The speed profile has a similar trend and is smoother with a more refined desired arrival time discretization (10 min instead of 30 min). However, the refined discretization is achieved at the cost of more computation time and data storage. Thus the 30 min discretization is used. See Appendix F for more details. Fig. 11(b) compares car speed for different objectives. When focusing on the total travel cost reduction, i.e., reducing the total travel cost, the TCS still allows mean speed reductions of more

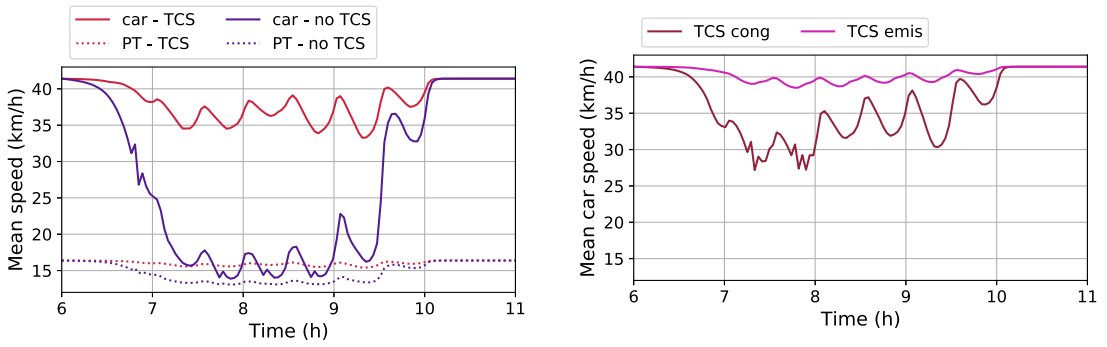

Fig. 11. Effect of the different dynamic TCS of the mean traffic speed: (a) mean car and PT speeds with dynamic TCS ('mid') and without TCS, and (b) mean car speed for the TCS 'cong' and 'emis'.

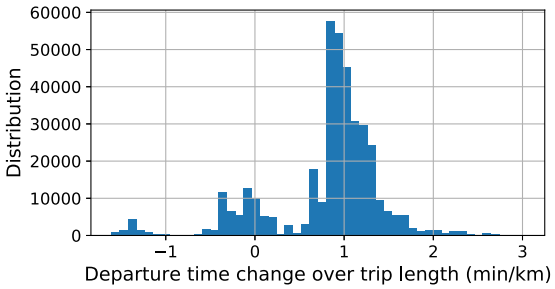

Fig. 12. Variations in departure time normalized by the trip length. A positive value means the traveler starts their trip later with TCS (scenario 'mid') than without.

than 10 km/h. In particular, the credit charge is low before 8:00, and the demand is already high; thus, the mean car speed is lower than after 8:00. The TCS designed for emission reduction keeps the mean speed around 40 km/h. This is expected as the emissions decrease with the mean car speed for the range of urban speeds.

The change in departure time per trip length between equilibrium without TCS and with TCS is computed in Fig. 12. Most travelers depart later with the TCS, about one minute per kilometer after their departures without TCS. Their travel times are reduced thanks to the better traffic conditions; thus, they leave later to arrive around their desired arrival time at their destinations. Some travelers depart earlier because they switch to modes with longer travel times (carpooling and PT).

We look at the effect of TCS on the different travelers. As we consider heterogeneous travelers in terms of desired arrival times, OD pairs, and VoT, it is crucial to look at the equity of the TCS. By looking at the distributions of the gains provided by the TCS ('mid'), we can quantify the number of travelers who are better or worse off with the policy proposed.

The gains are defined as the difference between travel costs (normalized or not by the VoT) with and without TCS. For a given set of traveler parameters (VoT, trip length, and desired arrival time), the TC gain Γ is the difference between the TC associated with the possible departure times and modes and weighted by the user distribution:

$$\Gamma = \frac{1}{d(c, i_l, i_{t_a})} \left(\sum_{i_{t_d}, m} f_{\text{no TCS}}(\omega) TC_{\text{no TCS}}(\omega) - f(\omega) TC(\omega) \right), \ \omega = (c, i_l, i_{t_a}, i_{t_d}, m), \ \forall \ (c, i_l, i_{t_a}). \tag{22}$$

A positive gain is favorable for the traveler as it means its average TC decreases with the TCS. The distributions of the TC gains are shown in Fig. 13. Most travelers are better off with the TCS in terms of normalized travel cost (by the VoT) and absolute travel costs. The majority see their TC equivalent decrease by 0 to 6 min (Fig. 13(a)) and 0 to 2 EUR (Fig. 13(b)). Wealthier travelers (higher VoT) are even better off since they will more readily buy credits to drive a car when the traffic conditions improve. The worst-off travelers lose the equivalent of several minutes with the TCS. Their TC increases by up to 1.6 EUR. The travelers who are better off decrease their TC by up to 14.7 EUR.

Let us have a look at the impact of the credit market. The trade gains from the market and the user cost gains (sum of travel cost and trade gains) are represented in Fig. 14. A positive trade gain means the traveler earns money by selling credits, while a negative gain means they spend money to buy credits. Fig. 14(a) gives an overview of the market outcomes. Travelers with a high VoT tend to buy credits from travelers with a smaller VoT; thus, they earn less money through the market. A traveler can earn around 0.8 EUR by riding PT and spend around 5.4 EUR driving their car alone during the highest charging period. When weighting the trade gains by the user distribution, some travelers spend up to 4 EUR. In contrast, others earn up to 0.7 EUR, depending on

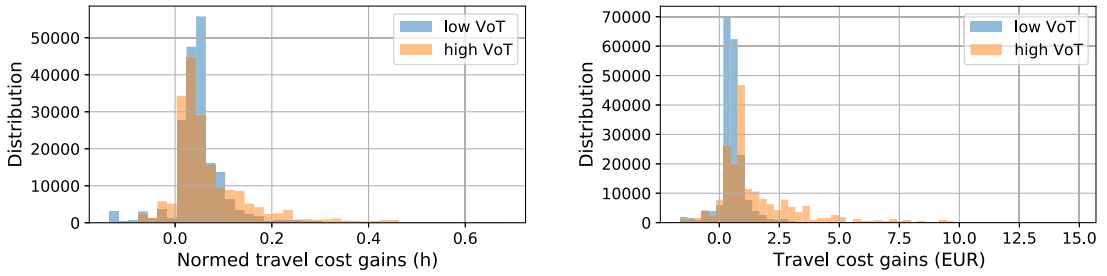

(a) (b)

Fig. 13. Distribution of the travel cost gains: (a) normalized by the VoT and (b) absolute travel cost.

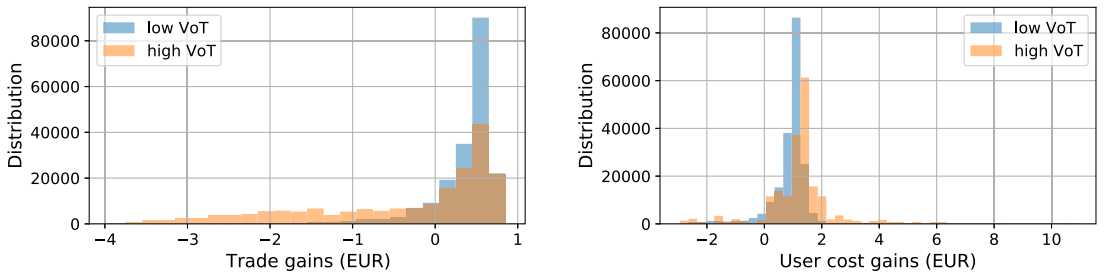

(a) (b)

Fig. 14. Distribution of the benefits of the TCS: (a) trade gains (money earned or spent through the market) and (b) user cost gains.

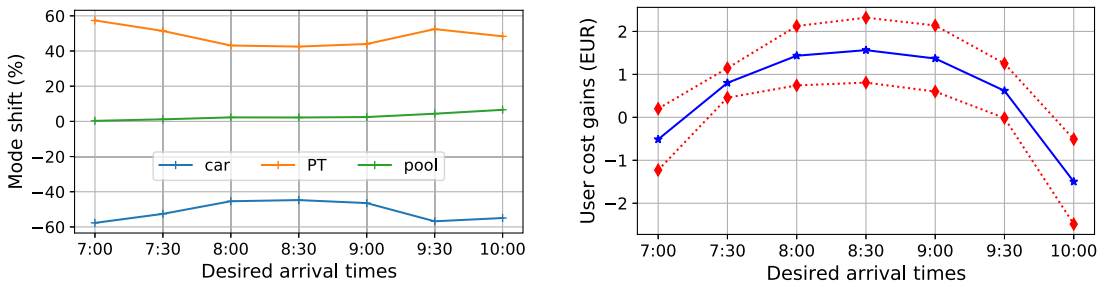

(a) (b)

Fig. 15. (a) Mode shift and (b) user cost gains with respect to the desired arrival times. The blue line is the average, and the red lines are the average plus/minus the standard deviation.

their characteristics (VoT, trip length, and desired arrival time). The effect of TCS on the user cost (travel cost plus credit trade) is represented in Fig. 14(b). Most travelers are better off with the TCS, as they decrease their user costs by 0 to 2 EUR. About 6% of the travelers see their user costs increase with this TCS, meaning 94% benefit from the TCS. The worst off lose 2.9 EUR, while those better off earn up to 10.8 EUR. Note that those estimations do not account for the benefits linked to lower pollution levels, such as better air quality.

The TCS has different impacts on different travelers. We investigate the relationship between desired arrival times, the mode shift, i.e., the evolution of modal shares between before and after TCS (scenario 'mid'), and the user cost gains in Fig. 15. The mode shift (Fig. 15(a)) from car to PT is more pronounced for travelers wanting to arrive outside the demand peak (before 7:30 or after 9:30), when up to 57% of the travelers leave their car to ride PT. Around 45% of the travelers with desired arrival times during the peak hour (between 8:00 and 9:00) switch from their cars to PT. This seems counterintuitive as the credit charge is higher during peak hours. The traffic conditions are bad during peak hours without TCS, and the car share is already lower than during peak hours. The user cost gain is positive for peak-hour users and negative for off-peak travelers (Fig. 15(b)). On-peak commuters benefit from better traffic conditions, which outweighs the burden of the TCS (mode shift or credit buy). On the contrary, the traffic conditions are already satisfying off-peak, and the slight improvement thanks to TCS does not outweigh additional TCS costs. We provide a similar analysis for the trip lengths in Fig. 16.

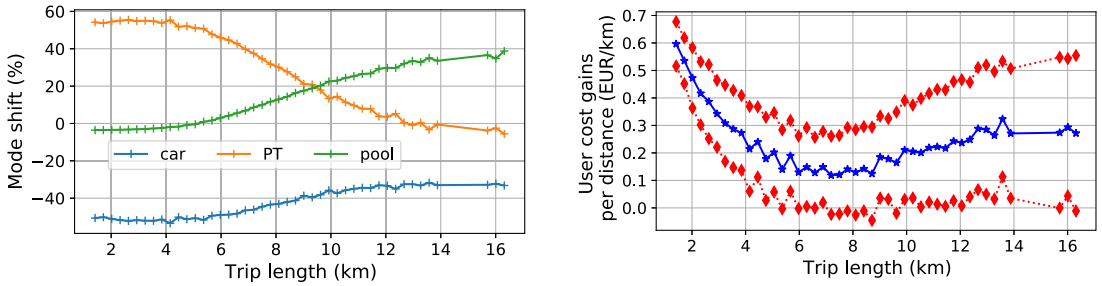

(a) (b)

Fig. 16. (a) Mode shift and (b) user cost gains per distance with respect to trip lengths. The blue line is the average, and the red lines are the average plus/minus the standard deviation.

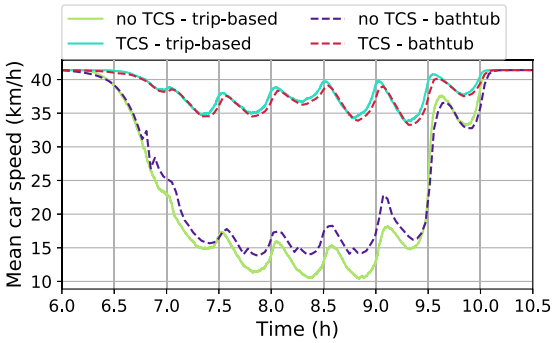

Fig. 17. Comparison of the mean car speeds with and without TCS for the bathtub and trip-based MFD resolutions.

Travelers with short and long trips change modes differently with the TCS (Fig. 16(a)). For trips shorter than 6 km, the modal shift is almost exclusively from cars to PT, with 50% to 55% of the demand switching from cars to PT. On the contrary, for trips longer than 10 km, more travelers stick to solo car driving and prefer carpooling to PT. The mode share of solo car drivers decreases by only 32 to 33 points. The carpooling share increases by up to 39 points. Sharing a car ride is attractive for long trips. The extra costs (waiting time and credit charge) do not depend on the trip length. The user cost gains per distance (Fig. 16(b)) are, on average, positive for the range of trip lengths in this case study. Short trips tend to benefit more from the TCS, as those travelers tend to shift towards PT and earn money by selling credits.

4.3. Comparison with the trip-based MFD

We compute the trip-based MFD simulation for the reference test case without TCS and the intermediate 'mid' TCS to assess the discretization effects. The trip-based MFD, via its event-based resolution, provides the exact computation of the arrival times. It can be viewed as the plant model. It does not use any discretization. It is, however, significantly more time-consuming to compute the arrival times for a given assignment than the discretization of the bathtub. Typically, the computation time is longer by three orders of magnitude. The trip lengths are those from the continuous demand before the discretization. The departure times are smooth: the trip linked to a departure time index i_{t_d} in the bathtub corresponds to a departure time randomly drawn from the uniform distribution $[(i_{t_d} - 0.5)\Delta_t, (i_{t_d} + 0.5)\Delta_t]$. We only consider trips with a user distribution more than one traveler. Less than 2% of the travel demand is lost in the process. The mean car speeds are compared in Fig. 17. Some deviations, up to 4 km/h for car speed, can be observed in the no TCS case between the network speed in the MFD and the bathtub. Due to the affine transformation of Eq. (21), the PT speed error is below 0.5 km/h. The differences are barely noticeable with TCS. The generalized bathtub tends to underestimate the congestion.

To quantify the error made in congestion and pollution estimation with the bathtub, we compare the TCS and the carbon emissions both with and without TCS in Fig. 18. The errors stay below 3% for total travel cost (Fig. 18(a)) and 11% for carbon emissions (Fig. 18(b)). The numerical approximations of the multimodal generalized bathtub are below the differences between the scenarios with and without TCS. The numerical resolution of the bathtub still gives a reasonable quantification of the economic and environmental benefits of the TCS at a lower computational cost than the trip-based MFD. The trip-based approach thus validates the departure time and trip length discretization choices: the respective precisions of 145 s and 304 m.

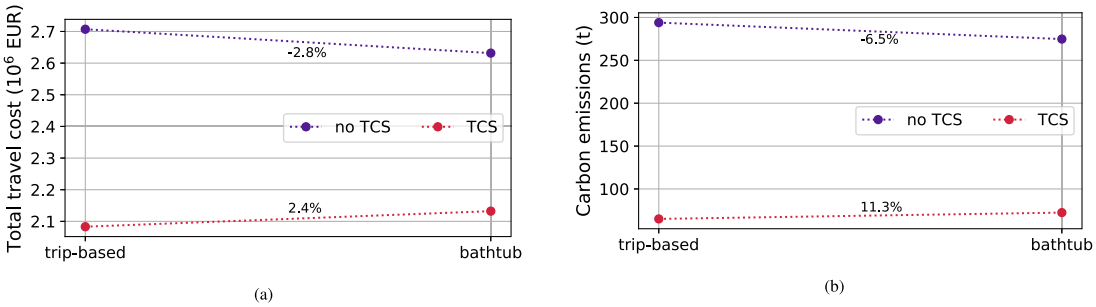

Fig. 18. Variations of the objectives measures between the bathtub and trip-based MFD: (a) total travel cost and (b) carbon emission.

5. Conclusion

During the last two decades, the literature has provided improvements to the bottleneck model in order to better quantify the economic losses caused by congestion. It also allowed us to better understand the potential benefits of demand management policies such as congestion pricing and Tradable Credit Schemes (TCS). The main means of action was spreading departure times. Here, we formulated a multimodal generalized bathtub to account for different types of vehicles and transportation modes. Each traveler's choices consist of mode and departure times. We add a TCS to foster mode shifts during the peak hour. Public Transportation (PT) users ride for free, solo car drivers pay the total charge, and carpoolers only half. We computed the Stochastic User Equilibrium (SUE) to account for the uncertainty of users' choices. A realistic scenario based on the morning commute in Lyon illustrated the methodology proposed.

The framework proposed makes it possible to compare the advantage of a dynamic TCS over a static one. The dynamic TCS accounts for the different demand levels depending on the time of day. It permits a better reduction of the total travel cost, i.e., the sum of all travelers' travel costs. The SUE is based on travel cost; thus, the shift of travelers' departure time is relatively limited. The biggest impact is the mode shift: PT and carpooling mode shares increase at the expense of the car share. We drew a Pareto front to present how TCS can lead to different total travel cost and carbon emission compromises. A TCS named 'cong' led to low total travel cost; another named 'emis' permitted significant carbon reduction, and 'mid' was a trade-off between both measures.

As TCS is a policy involving a marketplace and trading commodities (in this case credits), it raises the question of individual gains when people have different VoTs (different economic classes). The results showed no significant disadvantage for one category of VoT. With the 'mid' TCS, more than 94% of the population benefited from the TCS, as it reduced their user costs. However, it did not account for environmental aspects like air quality or noise. The numerical resolution of the multimodal generalized bathtub approximated the travel times. A comparison with the exact solution via trip-based MFD showed that the numerical error was below the order of benefits of the TCS. Moreover, the methodology proposed was shown to efficiently assess and optimize the benefits of TCS. The framework used the advantages of macroscopic simulation to reduce the need for computation power and data collection.

Further steps in the evaluation of dynamic TCS will include the validation of traffic simulation through micro-simulation, the estimation of travelers' behavior and acceptance through surveys, and the acquisition of experimental data through pilot experiments.

CRediT authorship contribution statement

Louis Balzer: Conceptualization, Data curation, Formal analysis, Investigation, Methodology, Visualization, Writing – original draft, Writing – review & editing. **Mostafa Ameli:** Conceptualization, Formal analysis, Investigation, Methodology, Project administration, Supervision, Writing – original draft, Writing – review & editing. **Ludovic Leclercq:** Conceptualization, Funding acquisition, Methodology, Project administration, Supervision, Writing – original draft, Writing – review & editing. **Jean-Patrick Lebacque:** Conceptualization, Formal analysis, Methodology, Supervision, Writing – original draft, Writing – review & editing.

Declaration of competing interest

The authors declare that they have no known competing financial interests or personal relationships that could have appeared to influence the work reported in this paper.

Data availability

Data will be made available on request.

Acknowledgment

This project has received funding from the European Union's Horizon 2020 research and innovation program under Grant Agreement no. 953783 (DIT4TraM).

Appendix A. Multimodal generalized bathtub discretization

Since the solution is Lipschitz continuous, we approximate the solution $(z_m(t), H_m(t))$ as piece-wise linear functions calculated at nodal points. The numerical resolution of the bathtub requires the discretization of the trip length, departure time, and desired arrival times. The values of those discretized parameters and variables are identified by the following indexes:

$$\begin{cases} i_l = \lfloor (l - l_{\min})/\Delta_l + 0.5 \rfloor; \\ i_{t_d} = \lfloor t_d/\Delta_t + 0.5 \rfloor; \\ i_{t_a} = \lfloor (t_a - t_{a,\min})/\Delta_{t_a} + 0.5 \rfloor, \end{cases} \tag{A.1}$$

with $l_{\min}$ the minimum trip length and $t_{a,\min}$ the minimum desired departure time. $\lfloor x \rfloor$ is the integer part of x, i.e., the highest integer smaller than x. The first admissible departure time is taken as reference, i.e., is zero. The simulation time shares the same discretization as the departure times.

One can come back to the continuous value of the variables from the indexes:

$$\begin{cases} l = l_{\min} + i_l \Delta_l; \\ t = i_t \Delta_t; \\ t_a = t_{a,\min} + i_{t_a} \Delta_{t_a}. \end{cases} \tag{A.2}$$

In the rest of the paper, we use both the discrete and continuous formulations for the arguments of the functions interchangeably. The discrete versions of the demand and the assignment are defined by:

$$\begin{cases} d(c, i_l, i_{t_a}) & = \int_{\Theta(i_{t_a})} \int_{\Theta(i_l)} d(c, l, t_a) \mathrm{d}t_a \mathrm{d}l; \\ f(c, i_l, i_{t_a}, i_{t_d}, m) & = \int_{\Theta(i_{t_a})} \int_{\Theta(i_l)} \int_{\Theta(i_{t_d})} f(c, l, t_a, t_d, m) \mathrm{d}t_a \mathrm{d}l \mathrm{d}t_d; \end{cases} \tag{A.3}$$

with

$$\begin{cases} \Theta(i_{t_a}) & = [t_{a,\min} + (i_{t_a} - 0.5)\Delta_{t_a}, t_{a,\min} + (i_{t_a} + 0.5)\Delta_{t_a}], \\ \Theta(i_l) & = [l_{\min} + (i_l - 0.5)\Delta_l, l_{\min} + (i_l + 0.5)\Delta_l], \\ \Theta(i_{t_d}) & = [(i_{t_d} - 0.5)\Delta_t, (i_{t_d} + 0.5)\Delta_t]. \end{cases} \tag{A.4}$$

$$\begin{cases} z_m(i_t) & = z_m(i_{t-1}) + \Delta_t v_m \left(\{ H_{m'}(i_{t-1}) + \sum_{c, i_{t_a}, i_l} f(c, i_l, i_{t_a}, i_t, m') \}_{m' \in \mathcal{M}} \right) \\ H_m(i_t) & = \sum_{i_{t_d} \le i_t} F_m \left(\max(0, \lfloor \frac{(z_m(i_t) - z_m(i_{t_d}) - l_{\min})}{\Delta_l} \rfloor), i_{t_d} \right) \\ F_m(i_l, i_{t_d}) & = \sum_{i_{l'} \ge i_l} \sum_{c, i_{t_a}} a_{i_{t_d}, i_{l'}} f(c, i_{l'}, i_{t_a}, i_{t_d}, m) \end{cases} \tag{A.5}$$

Recall that F_m is a density with respect to t_d. $F_m(i_l, i_{t_d})$ is defined as the integral of $F_m(l, t_d)$ over $\Theta(i_{t_d})$. z_m and H_m are initialized with zero. The second part of the first equation allows us to account for the accumulation due to the trips starting during the current time step i_t. It counterbalances the fact that the bathtub tends to underestimate the congestion compared to the exact solution (computed via the trip-based MFD framework). Without this correction, the underestimation can be significant: with the case study, the equilibrium without TCS based on the generalized bathtub corresponds to gridlock with the exact solution (trip-based MFD). Adding the accumulation of trips starting during the current time step does not increase the computation time and memory requirements. On the contrary, increasing the time discretization to reach a satisfying precision mobilizes more resources.

Appendix B. Travel demand conservation

As we modify the user distribution, we need to ensure the conservation of the travel demand (Eq. (8)). The total change of the user distributions from $\mathcal{F}$ is spread among the configurations not selected to be changed ($\bar{\mathcal{F}}$). We first need to ensure the sum of the unchanged user distributions $\bar{C}$ of $\bar{\mathcal{F}}$ (positive) is big enough to absorb the sum of the changes C of $\mathcal{F}$ (positive or negative) if we use the update coefficient $1/r$:

$$\begin{cases} C & = \sum_{\omega \in \mathcal{F}} \frac{1}{r} (d(\omega)\psi(\omega) - f(\omega)); \\ \bar{C} & = \sum_{\omega \in \bar{\mathcal{F}}} f(\omega). \end{cases} \tag{B.1}$$

If $\bar{C}$ is larger than C, then we can use the update factor $\mu = 1/r$ as we can ensure the demand conservation by counterbalancing the deviation from the demand d using $\bar{\mathcal{F}}$. If it is not the case, the update factor μ is scaled down:

$$\begin{cases} \mu = \frac{1}{r} & \text{if } \bar{C} \ge C; \\ \mu = \frac{\bar{C}}{C} \frac{1}{r} & \text{if } \bar{C} < C. \end{cases} \tag{B.2}$$

Table D.1
Sensitivity of the carpooling penalty.

Penalty (min)	5	10 (ref)	15
Car solo share (%)	5.4	11.2	11.9
PT share (%)	74.2	79.9	80.6
Carpool share (%)	20.4	8.9	7.5
Total travel cost change (%)	−2.8	–	+2.5
Carbon emissions change (%)	−4.3	–	+0.7
Price change (%)	+9.4	–	0

The user distribution update follows:

$$\begin{cases} f_{\text{new}}(\omega) &= (1-\mu) f(\omega) + \mu d(\omega)\psi(\omega), \ \forall \omega \in \mathcal{F}; \\ f_{\text{new}}(\omega) &= \left(1 - \frac{C}{\bar{C}}\right) f(\omega), \ \forall \omega \in \bar{\mathcal{F}}. \end{cases} \tag{B.3}$$

It means we use $1/r$ as an update factor, except if the change quantity C is higher than the unchanged one $\bar{C}$. In this case, we cannot ensure the demand conservation without scaling down the update factor μ.

Appendix C. Algorithm for credit charge optimization

```
// Update the charging period with the largest absolute gradient.
for Each time period W do
    Compute the gradient of objective function according to Eq. (20);
end
Select the charging period W* with the highest absolute gradient |Obj_{W*}|;
if Obj_{W*} < 0 then
    τ(W*) ← τ(W*) + κ;
else
    τ(W*) ← max(τ(W*) − κ, κ);
end
// Prevent large variations between two consecutive charging periods.
for All previous charging periods W < W*, in a decreasing order do
    if τ(W) < τ(W + 1) − κ then
        τ(W) ← τ(W + 1) − κ;
    end
    if τ(W) > τ(W + 1) + κ then
        τ(W) ← τ(W + 1) + κ;
    end
end
for All later charging periods W > W*, in an increasing order do
    if τ(W) < τ(W − 1) − κ then
        τ(W) ← τ(W − 1) − κ;
    end
    if τ(W) > τ(W − 1) + κ then
        τ(W) ← τ(W − 1) + κ;
    end
end
```

Algorithm 1: Update of the credit charging profile.

Appendix D. Sensitivity of the carpooling penalty

Our case study is based on the assumption of a 10 min-penalty for carpoolers. This value is uncertain, and some additional traffic policies may decrease it, e.g., HOV lanes and carpooling parking places. We study the sensitivity of our case study with regard to the carpooling penalty. We compute the SUE for the intermediate TCS 'mid' with different values for the carpooling penalty ζ_{pool}: 5, 10 (reference case), and 15 min. The evolution of the carpooling shares is presented in Fig. D.1.

As expected, the carpool share increases as the penalty decreases. However, the difference between the 10 to 15 min penalty is small compared to the change between 5 and 10 min. We highlight the effects on other measures: modes shares, total travel cost, carbon emissions, and credit price (see Table D.1).

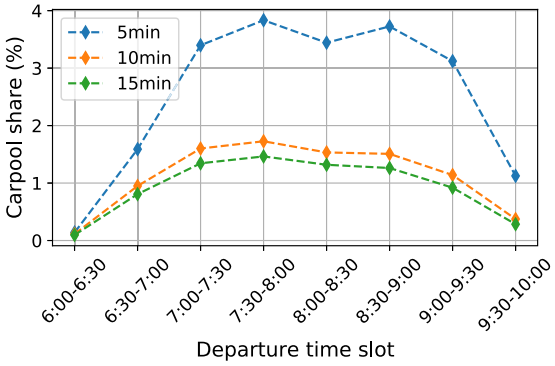

Fig. D.1. Carpooling shares for the different carpooling penalties.

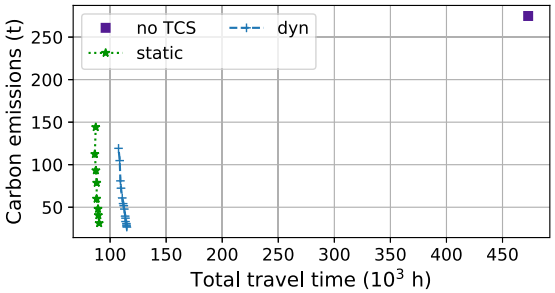

Fig. E.2. Total travel time vs. carbon emissions for different static and dynamic TCS. The reference case (no TCS) is also presented.

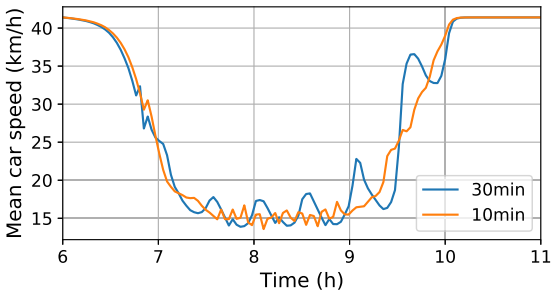

Fig. F.3. Comparison of the mean car speed for the 30-min (reference) and 10-min desired arrival time discretization.

The carpooling share decreases when the penalty increases, and both PT and car (solo) share increase. The effects on the system are not easy to predict: on one side, fewer carpoolers mean fewer cars, but on the other side, part of the former carpoolers may switch to solo car drivers. Compared to the reference case of a 10 min-penalty, the total travel cost and the carbon emissions increase marginally with the penalty. The credit price decreases by about 10% with 5 min and stays the same between 10 and 15 min. In conclusion, the effect of the carpooling penalty stays marginal, as even a variation of ± 5 min (50%) leads to small changes (2.5% and less) in the leading indicators: total travel cost, carbon emissions, and credit price.

Appendix E. Total travel time and carbon emissions

The differences between no TCS, static, and dynamic TCS in terms of total travel time and carbon emissions are presented in Fig. E.2. Both static and dynamic approaches reduce total travel time and carbon emissions. Static TCS allows for better compromises between total travel time and carbon emissions than dynamic schemes. The reason is that the dynamic schemes are designed to minimize the total travel costs. This objective function considers early/late arrival costs and travel time. Furthermore, the travelers choose their departure time and travel mode based on their user costs: travel time plus early/late cost plus TCS-induced costs.

Appendix F. Sensitivity of the desired arrival time discretization

The coarse desired arrival time discretization creates waves in the average car and PT speed profiles (Fig. 11). We compute the SUE without TCS with a desired arrival time discretization of 10 min (against 30 min for the reference scenario) to assess the model's sensitivity to the discretization. The mean car speeds for both discretizations are compared in Fig. F.3. The speed profile is smoother with the 10 min. However, the global trend stays the same as the 30 min discretization. The speed in the congested regime is about 15 km/h for both cases.

References

Ameli, M., 2019. Heuristic Methods for Calculating Dynamic Traffic Assignment (Ph.D. thesis). IFSTTAR Paris and Université de Lyon.

Ameli, M., Faradonbeh, M.S.S., Lebacque, J.-P., Abouee-Mehrizi, H., Leclercq, L., 2022. Departure Time Choice Models in Urban Transportation Systems Based on Mean Field Games. Transp. Sci. http://dx.doi.org/10.1287/TRSC.2022.1147, URL: https://pubsonline.informs.org/doi/abs/10.1287/trsc.2022.1147.

Ameli, M., Lebacque, J.P., Leclercq, L., 2020. Cross-comparison of convergence algorithms to solve trip-based dynamic traffic assignment problems. Comput.-Aided Civ. Infrastruct. Eng. 35 (3), 219–240.

Ameli, M., Lebacque, J.P., Leclercq, L., 2021. Computational Methods for Calculating Multimodal Multiclass Traffic Network Equilibrium: Simulation Benchmark on a Large-Scale Test Case. J. Adv. Transp. 2021, http://dx.doi.org/10.1155/2021/8815653.

Arnott, R., 2013. A bathtub model of downtown traffic congestion. J. Urban Econ. 76 (1), 110–121. http://dx.doi.org/10.1016/j.jue.2013.01.001.

Arnott, R., Buli, J., 2018. Solving for equilibrium in the basic bathtub model. Transp. Res. B 109, 150–175. http://dx.doi.org/10.1016/j.trb.2017.12.003.

Arnott, R., de Palma, A., Lindsey, R., 1990. Economics of a bottleneck. J. Urban Econ. 27 (1), 111–130. http://dx.doi.org/10.1016/0094-1190(90)90028-L.

Balzer, L., Leclercq, L., 2022. Modal equilibrium of a tradable credit scheme with a trip-based MFD and logit-based decision-making. Transp. Res. C 139, 103642. http://dx.doi.org/10.1016/J.TRC.2022.103642, URL: https://linkinghub.elsevier.com/retrieve/pii/S0968090X22000857.

Bao, Y., Verhoef, E.T., Koster, P., 2019. Regulating dynamic congestion externalities with tradable credit schemes: Does a unique equilibrium exist? Transp. Res. B 127, 225–236. http://dx.doi.org/10.1016/j.trb.2019.07.012.

Chu, X., 1995. Endogenous Trip Scheduling: The Henderson Approach Reformulated and Compared with the Vickrey Approach. J. Urban Econ. 37 (3), 324–343. http://dx.doi.org/10.1006/juec.1995.1017, URL: https://linkinghub.elsevier.com/retrieve/pii/S0094119085710170.

Dakic, I., Yang, K., Menendez, M., Chow, J.Y., 2021. On the design of an optimal flexible bus dispatching system with modular bus units: Using the three-dimensional macroscopic fundamental diagram. Transp. Res. B 148, 38–59. http://dx.doi.org/10.1016/J.TRB.2021.04.005.

Fosgerau, M., 2015. Congestion in the bathtub. Econ. Transp. 4, 241–255. http://dx.doi.org/10.1016/j.ecotra.2015.08.001.

Fosgerau, M., Small, K.A., 2013. Hypercongestion in downtown metropolis. J. Urban Econ. 76 (1), 122–134. http://dx.doi.org/10.1016/j.jue.2012.12.004.

Gao, G., Sun, H., 2014. Internalizing Congestion and Emissions Externality on Road Networks with Tradable Credits. Procedia - Soc. Behav. Sci. 138, 214–222. http://dx.doi.org/10.1016/j.sbspro.2014.07.198.

HERE Developer, 2020. URL: https://developer.here.com/.

Jia, Z., Wang, D.Z., Cai, X., 2016. Traffic managements for household travels in congested morning commute. Transp. Res. E: Logist. Transp. Rev. 91, 173–189. http://dx.doi.org/10.1016/j.tre.2016.04.005.

Jin, W.L., 2020. Generalized bathtub model of network trip flows. Transp. Res. B 136, 138–157. http://dx.doi.org/10.1016/j.trb.2020.04.002.

Lamotte, R., Geroliminis, N., 2018. The morning commute in urban areas with heterogeneous trip lengths. Transp. Res. B 117, 794–810. http://dx.doi.org/10.1016/j.trb.2017.08.023.

Lebacque, J.-P., Ameli, M., Leclercq, L., 2022. Stochastic departure time user equilibrium with heterogeneous trip profile. In: The 10th Symposium of the European Association for Research in Transportation. HEART, URL: https://hal.archives-ouvertes.fr/hal-03680843/document.

Leclercq, L., Sénécat, A., Mariotte, G., 2017. Dynamic macroscopic simulation of on-street parking search: A trip-based approach. Transp. Res. B 101, 268–282. http://dx.doi.org/10.1016/j.trb.2017.04.004.

Lejri, D., Can, A., Schiper, N., Leclercq, L., 2018. Accounting for traffic speed dynamics when calculating COPERT and PHEM pollutant emissions at the urban scale. Transp. Res. D 63, 588–603. http://dx.doi.org/10.1016/j.trd.2018.06.023.

Li, Z.C., Huang, H.J., Yang, H., 2020. Fifty years of the bottleneck model: A bibliometric review and future research directions. Transp. Res. B 139, 311–342. http://dx.doi.org/10.1016/j.trb.2020.06.009.

Lindsey, R.C., Van den Berg, V.A., Verhoef, E.T., 2012. Step tolling with bottleneck queuing congestion. J. Urban Econ. 72 (1), 46–59. http://dx.doi.org/10.1016/j.jue.2012.02.001.

Liu, R., Chen, S., Jiang, Y., Seshadri, R., Ben-Akiva, M., Azevedo, C.L., 2022. Managing network congestion with a trip- and area-based tradable credit scheme. Transp. B: Transp. Dyn. 1–29. http://dx.doi.org/10.1080/21680566.2022.2083034, URL: https://www.tandfonline.com/doi/abs/10.1080/21680566.2022.2083034.

Loder, A., Ambühl, L., Menendez, M., Axhausen, K.W., 2017. Empirics of multi-modal traffic networks – Using the 3D macroscopic fundamental diagram. Transp. Res. C 82, 88–101. http://dx.doi.org/10.1016/j.trc.2017.06.009.

Loder, A., Bressan, L., Wierbos, M.J., Becker, H., Emmonds, A., Obee, M., Knoop, V.L., Menendez, M., Axhausen, K.W., 2021. How Many Cars in the City Are Too Many? Towards Finding the Optimal Modal Split for a Multi-Modal Urban Road Network. Front. Future Transp. 5. http://dx.doi.org/10.3389/FFUTR.2021.665006.

Loder, A., Dakic, I., Bressan, L., Ambühl, L., Bliemer, M.C., Menendez, M., Axhausen, K.W., 2019. Capturing network properties with a functional form for the multi-modal macroscopic fundamental diagram. Transp. Res. B 129, 1–19. http://dx.doi.org/10.1016/j.trb.2019.09.004.

Mariotte, G., Leclercq, L., Laval, J.A., 2017. Macroscopic urban dynamics: Analytical and numerical comparisons of existing models. Transp. Res. B 101, 245–267. http://dx.doi.org/10.1016/j.trb.2017.04.002.

Miralinaghi, M., Peeta, S., He, X., Ukkusuri, S.V., 2019. Managing morning commute congestion with a tradable credit scheme under commuter heterogeneity and market loss aversion behavior. Transp. B 7 (1), 1780–1808. http://dx.doi.org/10.1080/21680566.2019.1698379, URL: https://www.tandfonline.com/doi/abs/10.1080/21680566.2019.1698379.

Nie, Y.M., 2015. A New Tradable Credit Scheme for the Morning Commute Problem. Netw. Spat. Econ. 15 (3), 719–741. http://dx.doi.org/10.1007/s11067-013-9192-8, URL: http://www.tfl.gov.uk/tfl/roadusers/congestioncharge/whereandwhen/.

Nie, Y.M., Yin, Y., 2013. Managing rush hour travel choices with tradable credit scheme. Transp. Res. B 50, 1–19. http://dx.doi.org/10.1016/j.trb.2013.01.004.

Ntziachristos, L., Gkatzoflias, D., Kouridis, C., Samaras, Z., 2009. COPERT: A European road transport emission inventory model. Environ. Sci. Eng. (Subseries: Environmental Science) 491–504. http://dx.doi.org/10.1007/978-3-540-88351-7{_}37, URL: https://link.springer.com/chapter/10.1007/978-3-540-88351-7_37.

Paipuri, M., Barmpounakis, E., Geroliminis, N., Leclercq, L., 2021. Empirical observations of multi-modal network-level models: Insights from the pNEUMA experiment. Transp. Res. C 131, 103300. http://dx.doi.org/10.1016/J.TRC.2021.103300.

Paipuri, M., Leclercq, L., 2020. Bi-modal macroscopic traffic dynamics in a single region. Transp. Res. B 133, 257–290. http://dx.doi.org/10.1016/j.trb.2020.01.007.

Sbayti, H., Lu, C.C., Mahmassani, H.S., 2007. Efficient implementation of method of successive averages in simulation-based dynamic traffic assignment models for large-scale network applications. Transp. Res. Rec. 2029 (1), 22–30.

Sheffi, Y., 1985. Urban Transportation Networks: Equilibrium Analysis with Mathematical Programming Methods. Prentice-Hall.

Tian, L.J., Yang, H., Huang, H.J., 2013. Tradable credit schemes for managing bottleneck congestion and modal split with heterogeneous users. Transp. Res. E Logist. Transp. Rev. 54, 1–13. http://dx.doi.org/10.1016/j.tre.2013.04.002.

Vickrey, W.S., 1969. Congestion Theory and Transport Investment. Source: Am. Econ. Rev. 59 (2), 251–260.

Vickrey, W., 2020. Congestion in midtown Manhattan in relation to marginal cost pricing. Econ. Transp. 21, 100152. http://dx.doi.org/10.1016/j.ecotra.2019.100152.

Xiao, L.L., Huang, H.J., Liu, R., 2015. Tradable credit scheme for rush hour travel choice with heterogeneous commuters. Adv. Mech. Eng. 7 (10), 168781401561243. http://dx.doi.org/10.1177/1687814015612430, URL: http://journals.sagepub.com/doi/10.1177/1687814015612430.

Xiao, L.L., Liu, T.L., Huang, H.J., 2016. On the morning commute problem with carpooling behavior under parking space constraint. Transp. Res. B 91, 383–407. http://dx.doi.org/10.1016/J.TRB.2016.05.014.

Xiao, L.L., Liu, T.L., Huang, H.J., 2021a. Tradable permit schemes for managing morning commute with carpool under parking space constraint. Transportation 48, 1563–1586. http://dx.doi.org/10.1007/s11116-019-09982-w, URL: https://link.springer.com/article/10.1007/s11116-019-09982-w.

Xiao, L.L., Liu, T.L., Huang, H.J., Liu, R., 2021b. Temporal-spatial allocation of bottleneck capacity for managing morning commute with carpool. Transp. Res. B 143, 177–200. http://dx.doi.org/10.1016/j.trb.2020.11.007.

Yang, H., Wang, X., 2011. Managing network mobility with tradable credits. Transp. Res. B 45 (3), 580–594. http://dx.doi.org/10.1016/j.trb.2010.10.002.

Yu, X., van den Berg, V.A., Verhoef, E.T., 2019. Carpooling with heterogeneous users in the bottleneck model. Transp. Res. B 127, 178–200. http://dx.doi.org/10.1016/j.trb.2019.07.003.